The Clusters of Nitrogenase: Synthetic Methodology in the Construction of Weak-Field Clusters

Sonny C. Lee*,† and R. H. Holm*

Department of Chemistry and Chemical Biology, Harvard University, Cambridge, Massachusetts 02138

Received June 3, 2003

Contents

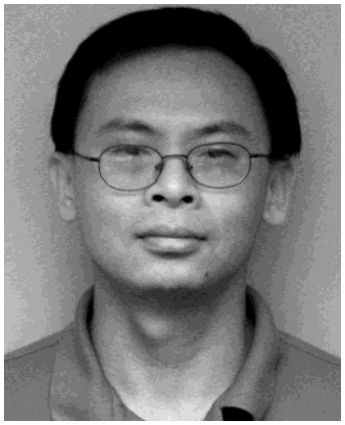

Sonny C. Lee was born in Ping-Tung, Taiwan, and received his formal education at the California Institute of Technology (B.S.), Harvard University (Ph.D. with R. H. Holm), and again at Caltech (postdoctoral fellowship with H. B. Gray). He has served on the faculty of the Department of Chemistry at Princeton University, where he was a Beckman Young Investigator and recipient of an NSF Career Award, and is currently a Visiting Scholar at Harvard. His research interests involve synthetic aspects of inorganic chemistry, including the cluster chemistry of weak-field iron with anionic nitrogen ligands and its relationship (maybe) to biological nitrogen fixation.

Richard H. Holm was born in Boston, MA, spent his younger years on Nantucket Island and Cape Cod, and graduated from the University of Massachusetts (B.S.) and Massachusetts Institute of Technology (Ph.D.). He has served on the faculties of the University of Wisconsin, the Massachusetts Institute of Technology, and Stanford University. Since 1980, he has been at Harvard University, where he has been Chair of the Department of Chemistry and, from 1983, Higgins Professor of Chemistry. His research interests are centered in inorganic and bioinorganic chemistry, with particular reference to the synthesis and properties of molecules whose structures and reactions are pertinent to biological processes.

1. Introduction

Among the more compelling challenges in the synthetic analogue approach to metalloprotein active sites is the construction of metal *clusters* that are meaningful representations of the products of biosynthesis. For iron−sulfur clusters of the types Fe_2S_2 (rhomboidal), Fe_3S_4 (cuboidal), and Fe_4S_4 (cubane-type), the goals of synthesis and property elucidation are largely met.[1] There remain, however, problems of greater complexity and allure for the synthetic inorganic chemist who chooses to pursue metal

† Visting Research Scholar, 2002−2004.

10.1021/cr0206216 CCC: $48.50
Published on Web 11/06/2003

Table 1. Bridged Biological Metal−Sulfur Assemblies

assembly[a]	refs
Sulfite Reductase	8, 9
$[Fe_4S_4]$-(μ_2-S_{Cys})-[Fe(siroheme)]	
[Fe]-Hydrogenase	10, 11
$[Fe_4S_4]$-(μ_2-S_{Cys})-$[Fe_2(\mu_2\text{-}CO)(\mu_2\text{-}(SCH_2XCH_2S)(CN)_2(CO)_2]$[d]	
[NiFe]-Hydrogenase	12−14
$(_{Cys}S)_2Ni(\mu_2\text{-}S_{Cys})_2Fe(CN)_2CO$	
Carbon Monoxide Dehydrogenase	
$[NiFe_3S_3]$-(μ_2-S)(μ_3-S)-$[Fe(N_{His})(S_{Cys})]$[b]	15
$[NiFe_3S_3]$-($\mu_{3(4)}$-S)(μ_2-S_{Cys})-$[Fe(N_{His})(S_{Cys})]$[b]	16
$[Fe_4S_4]$-(μ_2-S_{Cys})-$[M((\mu_2\text{-}S_{Cys})_2Gly)Ni]$[c]	
M = Cu	17
M = Ni, Zn	18
[(pyranopterindithiolate)MoO(OH)]-(μ_2-S)-$[Cu(S_{Cys})]$	19
Nitrogenase P Clusters	20, 21
P^N cluster: $[Fe_4S_3]$-(μ_2-S_{Cys})$_2$(μ_6-S)-$[Fe_4S_3]$	
P^{OX} cluster: $[Fe_4S_3]$-(μ_2-S_{Cys})$_2$(μ_4-S)-$[Fe_4S_3]$	
Nitrogenase FeMo-co Cluster	
$[Fe_4S_3]$-(μ_2-S)$_3$(μ_6-X)-$[MoFe_3S_3]$	20, 21, 23, 24
X = N, O (?)[d]	22

[a] Minimal formulations; most terminal ligands and incompletely defined ligands are omitted. [b] C cluster, site of CO/CO_2 interconversion. [c] A cluster, site of acetyl-CoA synthase activity; Cys-Gly-Cys peptide. [d] Identity of atom/group X uncertain.

clusters in biology. In metal−sulfur chemistry, unrealized objectives of synthesis exist within a broader class of protein-bound entities that we have termed "bridged biological metal assemblies".[2] These are constructs containing two or more discrete or recognizable fragments that are juxtaposed wholly or in part by one or more covalent bridges. Collected in Table 1 are the six most prominent examples of metal−sulfur bridged assemblies currently recognized, referenced in terms of protein structure. The molecular structures, presented in Figures 1 and 2, readily convey the descriptive term. All but [NiFe]-hydrogenases and Mo-containing carbon monoxide dehydrogenase accommodate clusters, either cuboidal (MFe_3S_3, Fe_4S_3) or cubane-type (Fe_4S_4), and all except Mo-CODH are iron−sulfur proteins. Some of these clusters have been prepared separately, but none has been obtained in the bridging configuration of a native site.

Two attributes of bridged assemblies seem clear. First, given the variation and distribution of these sites as currently understood, there can be little doubt that other native bridged sites of comparable or greater complexity remain to be discovered. Second, these sites are, or certainly are among, the most imposing synthetic challenges in bioinorganic chemistry. One need not reflect long to recognize that the synthetic methods available for the preparation of such complex metal arrays are limited, being sharply constrained by intrinsic chemical properties which include nonselective multisite reactivity, oxidative and electrophilic instability, and ligand (core and terminal) lability. These concerns are exacerbated by the typical biological combination of σ- and π-donor ligands (sulfur, nitrogen, oxygen) and 3d metals that renders the local metal centers high-spin, and therefore kinetically destabilized. These *weak-field* clusters are distinguished from *strong-field* examples, whose characteristics, dictated by the presence of low-spin metal sites, frequently include substantial kinetic stability, π-acceptor ligation, lower oxidation states, and direct metal−metal bonding; the only biological strong-field cluster known at present is the dinuclear portion of the [Fe]-hydrogenase active site. Taken together, these considerations mark the synthesis of analogues of bridged assemblies as a forefront area in contemporary bioinorganic chemistry.

This review delineates the pursuit of synthetic analogues to the bridged cluster assemblies within nitrogenase. The two clusters of interest, the P cluster and the FeMo-co cluster, share distinguishing features (Figure 2) that separate them from the other assemblies in Table 1. Both clusters are intimately bridged, compact assemblies consisting of cuboidal halves fused through a central atom with a μ_6 bridging modality found nowhere else in biology. The P cluster, in its as-isolated or P^N state, has a structure in which two Fe_4S_3 units are bridged by an uncommon μ_6-S atom and by two μ_2-S_{Cys} residues. Four terminal Fe−S_{Cys} interactions complete the cluster ligand set, and all iron sites possess distorted tetrahedral FeS_4 coordination. FeMo-co is built of Fe_4S_3 and $MoFe_3S_3$ fragments bridged by three μ_2-S atoms and one μ_6-X atom whose identity (C, N, or O) is uncertain at present. The cluster is anchored to the protein backbone by one Mo−N_{His} and one Fe−S_{Cys} bond. The seven iron sites have distorted tetrahedral geometry, while the molybdenum atom is six-coordinate with distorted octahedral MoS_3NO_2 coordination. The two cluster types lie within the $\alpha_2\beta_2$ MoFe protein ($M_r \approx 240\,000$) of the nitrogenase enzyme complex, with the P cluster occurring at the interface between the α- and β-subunits and FeMo-co bound inside the β-subunit. The current interpretation of cluster function assigns the P cluster as the electron acceptor from the obligate redox partner in the enzyme system (the reduced Fe protein); FeMo-co, in turn, accepts electrons from the P cluster and serves as the site of dinitrogen binding, activation, and reduction. Biological nitrogen fixation, in the form of reaction 1, and cluster and protein structural features have been extensively reviewed.[3−7]

$$N_2 + 8H^+ + 8e^- + 16ATP \rightarrow 2NH_3 + H_2 + 16ADP + 16P_i \quad (1)$$

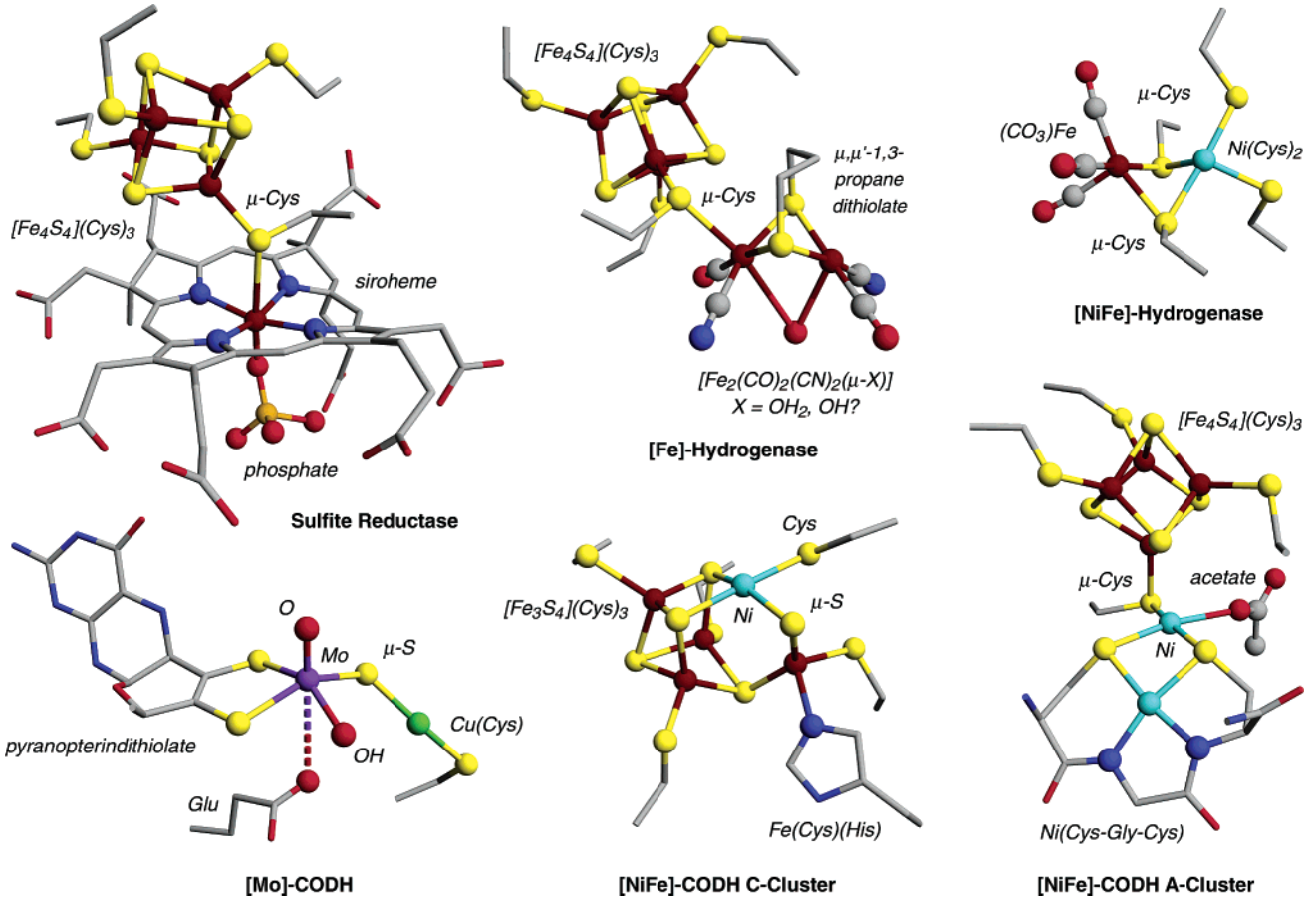

Figure 1. Structures of the bridged assemblies in sulfite reductase,[8] hydrogenases,[11,13] and carbon monoxide dehydrogenases,[15,18,19] shown to the same scale. Cluster cores, terminal donor atoms, and small ligands are represented as ball-and-stick models, and organic cofactors and amino acids as cylinders; amino acids and the pyranopterindithiolate ligand are truncated for clarity. Color convention: carbon, gray; nitrogen, blue; oxygen, red; phosphorus, orange; sulfur, yellow; iron, dark red; nickel, light blue; copper, green; molybdenum, purple.

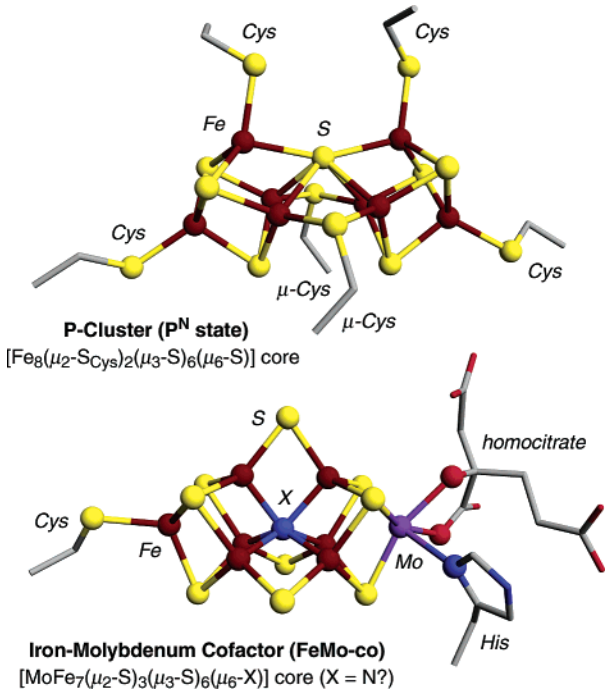

Figure 2. Structures of the clusters of nitrogenase in the dithionite-reduced states:[22] upper, the P^N cluster; lower, FeMo-co with interstitial atom X (shown here as nitrogen). Representation scale and conventions are the same as in Figure 1.

The history of iron−sulfur and metal−iron−sulfur clusters encountered over a ca. 25-year period of investigation, and considered pertinent in one respect or another to the ultimate synthesis and to the properties of the native clusters of nitrogenase, includes a variety of cluster types and contributions by a number of workers. We do not provide here a broad historical perspective but note instead certain areas of research and the work of several investigators. A large body of cluster synthesis research has been devoted to the creation of analogues to the heterometallic FeMo-co. At the beginning stages of the field, dinuclear and linear trinuclear clusters derived from $[MoS_4]^{2-}$, among them $[Cl_2FeS_2MoS_2]^{2-}$, $[(Cl_2Fe)S_2MoS_2(FeCl_2)]^{2-}$, $[Fe(S_2MoS_2)_2]^{3-}$, and related species, were the focus of extensive studies; summaries of early work are available.[25−27] Averill and co-workers[28−30] utilized linear clusters and also pursued a metal carbonyl synthetic approach leading to clusters such as $[MoFe_5S_6(CO)_6(PEt_3)_3]$, containing the $MoFe_3S_4$ cubane-type unit, and $[MoFe_6S_6(CO)_{16}]^{2-}$. Garner, Christou, et al.[31] provided significant early results on the synthesis and properties of weak-field $MoFe_3S_4$ clusters. The influential research by Coucouvanis and co-workers has spanned, inter alia, linear Mo−Fe−S clusters, molybdenum carbonyl-containing species such as $[(CO)_3MoFe_3S_4(SR)_3]^{3-}$ and $[Fe_6S_6(OR)_6(M(CO)_3)_2]^{3-}$, single- and double-cubane

$MoFe_3S_4$ clusters, and cuboidal strong-field $MoFe_3S_3$ carbonyl/phosphine clusters; some of this work has been summarized,[26,32,33] and a more recent narrative is forthcoming.[34]

In this review, emphasis is placed on synthetic methods, structures, and selected properties of clusters as developed and elucidated in the authors' laboratories. The field is described in three time frames: the X-ray absorption spectroscopy era, in which EXAFS analysis (1978) contributed the only concrete structural information; the macromolecular structure era, when crystallography (1992−1993) provided definition at increasingly higher resolution for the entire protein structure; and the ongoing interstitial atom era, when an atomic-resolution diffraction study (2002) revealed an interstitial atom inside FeMo-co, a structural component that had completely escaped all prior physicochemical interrogations. As will become evident, the construction of complete and faithful analogues of the electron-transfer P cluster and catalytic FeMo-co remains an imposing challenge that has yet to be met. The quest for these structures has nevertheless advanced inorganic cluster chemistry in directions that would have remained otherwise unexplored. This progress provides a philosophical justification, offered elsewhere,[35] for this speculative approach and serves as a preeminent demonstration of the increasing sophistication of the synthetic analogue strategy.

2. The XAS Era (1978–1992)

2.1. FeMo-co Bound and Free

A seminal event in the interpretation of nitrogenase structure and function was the demonstration by Shah and Brill[36] in 1977 that the MoFe protein contains a dissociable cofactor (FeMo-co) which could be extracted from the precipitated protein with NMF. When FeMo-co was added to a cofactor-deficient MoFe protein mutant, full activity was restored. The isolation and properties of FeMo-co in solution, as elucidated up to 1990, have been analyzed by Burgess.[37] Subsequently, evidence has been accumulated for cofactors in vanadium-containing (FeV-co) and all-iron (FeFe-co) nitrogenases.[5,6,38,39] An attractive proposal, advanced by several investigators and embodied in a recent theoretical treatment of spin-coupling,[40] is that vanadium and iron atoms occupy the core binding site of molybdenum, in which event the MFe_7S_9 cores are essentially isostructural. Vanadium EXAFS and other spectroscopic results are consistent with the proposal. So also is the ability of a hybrid protein formed from FeV-co and a cofactor-deficient MoFe protein to reduce the conventional test substrate acetylene to ethylene and a small amount of ethane, a property of native VFe proteins.[5,6,41] The hybrid protein does not reduce dinitrogen. The proposal awaits final confirmation by protein crystallography.

Cofactors have been obtained in solution; none has been isolated in substance. Nonetheless, their existence, dating from the original proof of FeMo-co, implies that they are potentially viable objects of synthesis and isolation. This is the basis for the synthetic analogue approach to the cofactors. P clusters have not been liberated intact from any protein, yet, as will be seen, the cofactor topology is accessible by synthesis.

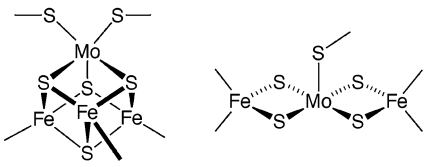

1 2

Figure 3. Structures proposed in 1978 for the molybdenum coordination environment in FeMo-co from Mo EXAFS of the reduced MoFe protein of *C. pasteurianum* nitrogenase.[43] Note that proposal **1** contains the $MoFe_3S_3$ fragment subsequently established in protein-bound FeMo-co by crystallography.

The first incisive structural results for metal sites in nitrogenase followed from an analysis of molybdenum EXAFS of the MoFe proteins from *Azotobacter vinelandii* and *Clostridium pasteurianum* in 1978. Hodgson and co-workers[42,43] demonstrated that the molybdenum coordination environments of the two lyophilized proteins and extracted FeMo-co are highly similar and proposed the partial structures **1** and **2** in Figure 3 for cofactor in the MoFe protein. Subsequent to that pioneering work,[43] molybdenum and iron EXAFS of native proteins and extracted cofactor demonstrated a sulfur-rich coordination environment for both elements and possible long-range Fe···Fe scattering at >3.5 Å, indicative of an extended structure beyond the Fe−Fe interactions at ca. 2.7 Å observed in all studies.[44−48] By 1987, the molybdenum EXAFS results for the *A. vinelandii* MoFe protein had converged to the following bond distances and coordination numbers:[47] Mo−S, 2.37(1) Å, 4.5; Mo−Fe, 2.68(1) Å, 3.5; Mo−O/N, 2.12(1) Å, 1.7. For FeMo-co extracted from this protein, the corresponding values were reported: Mo−S, 2.37(2) Å, 3.1; Mo−Fe, 2.70(2) Å, 2.6; Mo−O/N, 2.10(1) Å, 3.1. These latter results favor proposed structure **1** over **2** but neither support nor discount the full cubane-type geometry of **1**. As is now known, the $MoFe_3S_3$ cuboidal fragment of **1** is present in FeMo-co (Figure 2) and doubtless in free FeMo-co as well.

In the following sections, the early chemistry of Mo−Fe−S clusters with nuclearity four or higher is summarized, with emphasis on cluster types and their synthesis. The period covered is 1978−1992, although certain subsequent results extending from findings in this period are included. Here and elsewhere, spectroscopic and magnetic properties are not described in detail.

2.2. $MoFe_3S_4$ Double-Cubane Clusters

2.2.1. Self-Assembly

At the time of the FeMo-co structure proposals, synthetic methods for analogues of protein-bound iron−sulfur clusters had been developed.[49,50] In par-

Scheme 1. Synthetic Pathways to $[MoFe_3S_4]^{3+}$ Double Cubanes 1−4 by Self-Assembly, Fully Reduced Double Cubane 5, and Single Cubane 6 with an Exo Metal Bridged to the Molybdenum Atom

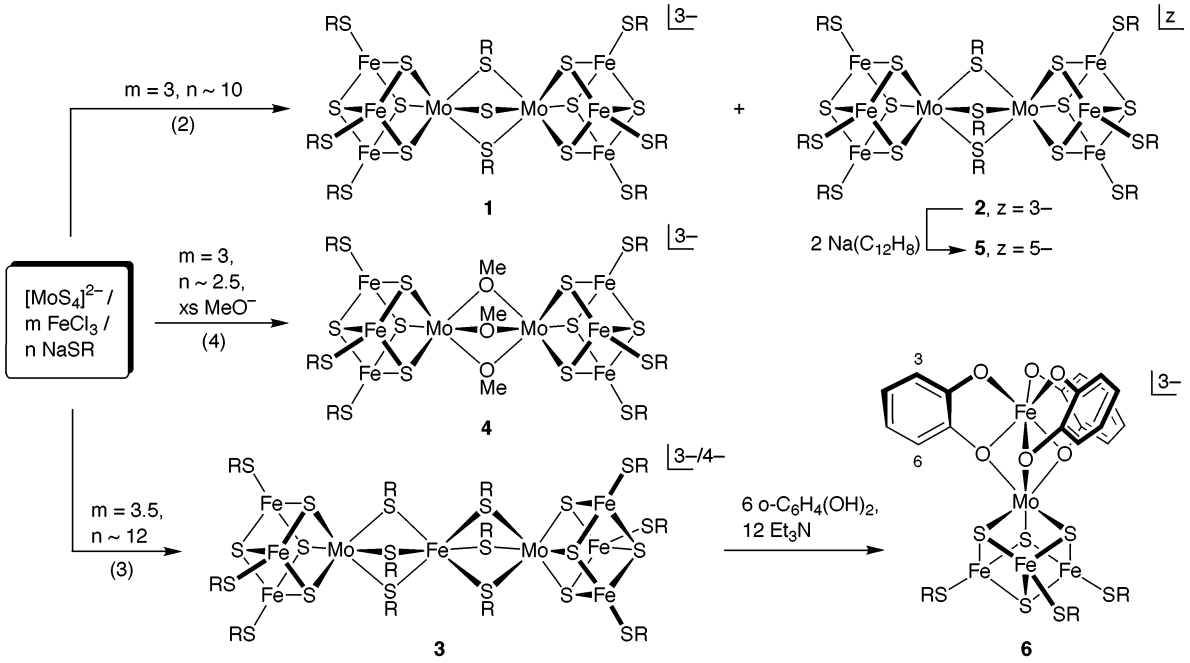

ticular, the spontaneous formation of $[Fe_4S_4(SR)_4]^{2-}$ clusters in high yield from simple reactants in the system $FeCl_3$/NaSH/NaSR in methanol[51,52] (and later in the system $FeCl_2$/S/NaSR[53]) suggested a self-assembly route to Mo−Fe−S clusters potentially related to FeMo-co. With knowledge of structure proposal **1**, one of us (R.H.H.) undertook the synthesis by self-assembly of Mo−Fe−S clusters. Leading results are summarized in Scheme 1. The reaction system $[MoS_4]^{2-}$/3$FeCl_3$/10NaSR afforded as its first characterized product the bis(thiolato)sulfido-bridged *double cubane* **1**.[54] Shortly thereafter, it was established that the assembly system afforded two additional double-cubane clusters, tris(thiolato)-bridged **2**[55] and $Fe(SR)_6$-bridged **3**.[56,57] Reaction stoichiometries and crystallization conditions were adjusted to allow the isolation of **1**−**3** as pure quaternary ammonium salts. The corresponding tungsten clusters have also been obtained in pure form. In the same period (1978−1980), Garner, Christou, and co-workers, using very similar systems, prepared more examples of cluster **2**. Further, they showed that, by using a smaller amount of thiolate and excess methoxide in methanol, the tris(methoxide)-bridged double cubane **4** (R = Ph) is formed.[58] The related cluster with R = Bu^t has been prepared in this laboratory.[59] The structures of **1**−**4** have been proven by crystallography. These are the first heterometal weak-field cubane-type clusters to have been prepared; their bridged topology had not been previously encountered.

The apparent stoichiometries of the complex assembly processes affording clusters **2**−**4** are given by reactions 2−4. Unlike the self-assembly of $[Fe_4S_4(SR)_4]^{2-}$, for which some of the component reactions leading to the cluster product have been identified,[60] there is no corresponding information on the pathway by which these clusters are assembled.

$$2[MoS_4]^{2-} + 6FeCl_3 + 17RS^- \rightarrow [Mo_2Fe_6S_8(SR)_9]^{3-} + 18Cl^- + 4RSSR \quad (2)$$

$$2[MoS_4]^{2-} + 7FeCl_3 + 20RS^- \rightarrow [Mo_2Fe_7S_8(SR)_{12}]^{3-} + 21Cl^- + 4RSSR \quad (3)$$

$$2[MoS_4]^{2-} + 6FeCl_3 + 14RS^- + 3MeO^- \rightarrow [Mo_2Fe_6S_8(OMe)_3(SR)_6]^{3-} + 18Cl^- + 4RSSR \quad (4)$$

Because isolated yields are often high (≳60%), the pathways must be ordered and the clusters abundantly stable thermodynamically. The clusters **2**, in particular, are frequently encountered in assembly systems based on $[MoS_4]^{2-}$ and directed toward other products. The assembly systems should be considered as redox-buffered, having a quantity of thiolate sufficient to adjust the core oxidation state to a stable level. Thus, in reaction 2, for example, eight electrons are required to reduce the reactants to the product containing two $[MoFe_3S_4]^{3+}$ cores. The electrons are supplied by 8 equiv of thiolate which appear among the products as four disulfides. The presence of a large excess of thiolate does not change the cluster oxidation state. However, lower oxidation states are accessible with stronger reductants. Cluster **2** is reducible by two electrons using sodium acenaphthylenide to yield $[Mo_2Fe_6S_8(SPh)_9]^{5-}$, which has been isolated and shown to retain the double-cubane arrangement (**5**, Scheme 1) with only slight dimensional changes.[59] In reaction 3, the oxidation state of the bridging iron atom, but not the cluster core, depends on the identity and quantity of thiolate. Clusters containing the selenide-substituted cores of **2** and **3** were prepared about 12 years later using analogous self-assembly systems based on $[MoSe_4]^{2-}$.[61]

Table 2. Electron-Transfer Series and Charge Distributions[a] in $[MFe_3S_4]$ Cubane Clusters (M = Mo, V)

$[MoFe_3S_4]^+$	↔	$[MoFe_3S_4]^{2+}$	↔	$[MoFe_3S_4]^{3+}$	↔	$[MoFe_3S_4]^{4+}$
$S = ?$		$S = 2$		$S = {}^3/_2$		$S = ?$
$[Mo^{3+}Fe^{2+}{}_3S_4]^+$		$[Mo^{3+}Fe^{2.33+}{}_3S_4]^{2+}$		$[Mo^{3+}Fe^{2.67+}{}_3S_4]^{3+}$		$[Mo^{3+}Fe^{3+}{}_3S_4]^{4+}$
		$[VFe_3S_4]^+$	↔	$[VFe_3S_4]^{2+}$	↔	$[VFe_3S_4]^{3+}$
		$S = 2$		$S = {}^3/_2$		$S = 0$
		$[V^{3+}Fe^{2+}{}_3S_4]^+$		$[V^{3+}Fe^{2.33+}{}_3S_4]^{2+}$		$[V^{3+}Fe^{2.67+}{}_3S_4]^{2+}$

[a] Iron oxidation states based on $\delta(^{57}Fe) = 1.51 - 0.41s$ (4.2 K) for tetrahedral FeS_4 sites;[1] M oxidation states obtained by difference.

2.2.2. Properties

Because of their uniqueness, clusters **1**−**4** were fascinating molecules for property elucidation. The clusters are strongly paramagnetic (5.7−5.8 μ_B at room temperature)[62] and display relatively sharp, isotropically shifted ^1H NMR spectra[57,58] that are useful in monitoring reactions. The properties of the clusters **2** have been the most thoroughly examined. Reactions 5 and 6 result in stepwise terminal ligand substitution[63] and are parallel to reactions of $[Fe_4S_4(SR)_4]^{2-}$ clusters.

$$[Mo_2Fe_6S_8(SR)_9]^{3-} + 6R'SH \rightarrow [Mo_2Fe_6S_8(SR)_3(SR')_6]^{3-} + 6RSH \quad (5)$$

$$[Mo_2Fe_6S_8(SR)_9]^{3-} + 6R'COCl \rightarrow [Mo_2Fe_6S_8(SR)_3Cl_6]^{3-} + 6R'COSR \quad (6)$$

Even with excess thiol or acid chloride, the bridging thiolates are not substituted. These reactions also apply to the clusters **3**. A later mechanistic study of acid-catalyzed substitution reactions at the iron sites of $[Mo_2Fe_6S_8(SEt)_9]^{3-}$ has led to the conclusion that the presence of the molybdenum atom enhances binding of CO or chloride compared to $[Fe_4S_4(SEt)_4]^{2-}$.[64] In an attempt to cleave a double-cubane to a single-cubane cluster, which had not been found among self-assembly reaction products, $[Mo_2Fe_7S_8(SEt)_{12}]^{3-}$ was treated with catechol/Et_3N (Scheme 1). The product was **6**, binding an *exo*-$[Fe(cat)_3]^{3-}$ group at the molybdenum site, rather than a simpler single cubane. Other $MoFe_3S_4$ clusters with exo-iron centers have been prepared recently.[65,66]

All clusters show well-defined electron-transfer behavior in the form of the three-member series 7.[57,59,63,67,68] Potentials follow a normal substituent dependence; for R = Ph, $E_{1/2} = -1.02$ and −1.23 V in DMF.[59] These and all subsequent potentials are quoted vs the SCE. These redox steps involve the core states $[MoFe_3S_4]^{2+,3+}$. The ^{57}Fe isomer shift difference

$$[Mo_2Fe_6S_8(SR)_9]^{5-} \leftrightarrow [Mo_2Fe_6S_8(SR)_9]^{4-} \leftrightarrow [Mo_2Fe_6S_8(SR)_9]^{3-} \quad (7)$$

between adjacent oxidation levels is 0.14−0.15 mm/s. From an empirical relationship available at the time between isomer shift δ and oxidation state s for tetrahedral FeS_4 coordination unit ($\delta = 1.44 - 0.43s$ at 4.2 K),[59] a difference of 0.43/3 = 0.14 mm/s is predicted if the difference electron is sequestered to the Fe_3S_4 core fragment. A more recent relationship based on a much larger database ($\delta = 1.51 - 0.41s$)[1] leads to the same conclusion. Charge distributions for the two core oxidation states are indicated in Table 2. A consistent property of these and all other $MoFe_3S_4$ clusters (vide infra) is that changes in electron density upon oxidation or reduction do appear to be largely confined to the Fe_3S_4 fragment.

The reduced clusters $[Mo_2Fe_6S_8(SPh)_9]^{5-}$ and $[Mo_2Fe_6S_8(SPh)_9]^{4-}$ (generated in solution by reaction of [3-] and [5-] clusters) evolve dihydrogen slowly from certain protic species, including PhSH and Et_3NH^+.[69] In DMA solutions containing 500 equiv of thiol, the [4-] and [5-] clusters, after 24 h, afford yields of 86% and ∼100% of dihydrogen, based on the reactions $2[4\text{-}] + 2H^+ \rightarrow 2[3\text{-}] + H_2$ and $[5\text{-}] + 2H^+ \rightarrow [3\text{-}] + H_2$, respectively. Experimental rate laws were established, and mechanisms were proposed. In contrast, $[Fe_4S_4(SPh)_4]^{3-}$, under the same conditions, gave a 42% yield. The results express the potential advantage of a two-electron carrier for the reduction of H^+ to hydride, which is then protonated to form H_2.

Much of the early work on double cubanes has been summarized.[70] Given that the cofactor molecule is mononuclear in molybdenum, a necessary next step was to obtain clusters with that property. The obvious goal was a single $MoFe_3S_4$ cluster which, because none had been detected among cluster assembly products, was sought by cleavage of double cubanes. Such clusters would ideally present a simpler problem in electronic structure and allow reactivity at both iron and molybdenum sites to be investigated.

2.3. $MoFe_3S_4$ Single-Cubane Clusters

The synthesis and reactions of single cubanes are outlined in Scheme 2. Key structures were established by crystallography. Utilizing $[W_2Fe_7S_8(SR)_{12}]^{3-}$ as the starting material, the tungsten analogues of nearly all clusters shown were also prepared and characterized. With few exceptions, formulas of single cubanes here and elsewhere are written with heterometal terminal ligands preceding M.

2.3.1. Synthesis from Double Cubanes

The structure of **6** suggested that a sufficiently large 3-substituent on the catechol ring could destabilize binding of the $[Fe(cat)_3]^{3-}$ fragment and lead to a single cubane without an exo metal. This objective was realized with 3,6-di-*n*-propyl- and 3,6-diallylcatechol,[71−73] and shortly thereafter with tetrachlorocatechol.[74] Reaction 8 affords the centrosymmetric double cubane **7** with two Mo−S(R)−Fe bridges. Bridge bond lengths are ca. 0.05−0.1 Å longer than terminal bond lengths in the same and related clusters, contributing to the ready formation of single cubane solvates **8** in solvolysis reaction 9. This reaction is complete in Me_2SO and DMF. As discovered much later, the R = Et cluster system in

Scheme 2. Formation of Single Cubanes 8−12 from Double Cubane 3[a]

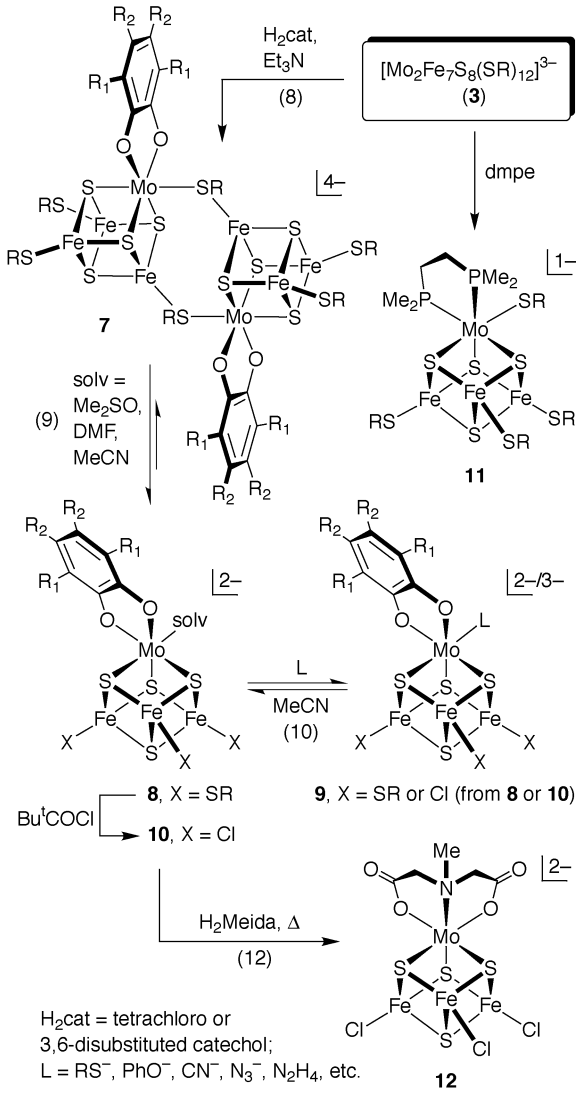

[a] Doubly bridged double cubane **7** is the immediate precursor to **8**−**10**. Reaction **12** has been extended to other diprotic chelate ligands (see text).

acetonitrile is in an equilibrium favoring the double cubane.[75] Certain clusters described in prior reports as acetonitrile solvates of single cubanes may have a similar equilibrium behavior. Treatment of **8** with various ligands in reaction 10 yields the ligated clusters **9**, which are subject to isolation with strongly binding ligands such as RS^-, PhO^-, and CN^-.[73,74,76]

$$[Mo_2Fe_7S_8(SR)_{12}]^{3-} + 5H_2cat + 10Et_3N \rightarrow [Mo_2Fe_6(cat)_2(SR)_6]^{4-} + [Fe(cat)_3]^{3-} + 10Et_3NH^+ + 6RS^- \quad (8)$$

$$[Mo_2Fe_6(cat)_2(SR)_6]^{4-} + 2solv \rightleftarrows 2[(cat)(solv)MoFe_3S_4(SR)_3]^{2-} \quad (9)$$

$$[(cat)(solv)MoFe_3S_4(SR)_3]^{2-} + L^{0/1-} \rightleftarrows [(cat)LMoFe_3S_4(SR)_3]^{2-/3-} + solv \quad (10)$$

Thus, the reaction sequence from **3** to **9** does afford the desired single cubanes. It is, however, somewhat laborious, requiring at least one week including the preparation of initial cluster **3**. Reaction of **3** (R = Et) with dmpe is simpler and produces the single cubane **11** in 33% yield.[77] Reaction of this cluster with excess benzoyl chloride caused rapid thiolate/chloride substitution at the iron sites, followed by a much slower substitution at the molybdenum site, resulting in $[(dmpe)ClMoFe_3S_4Cl_3]^{1-}$. These clusters have not been further investigated.

2.3.2. Self-Assembly

Following the synthesis of clusters **8**−**10**, the first examples of self-assembled $MoFe_3S_4$ single cubanes were reported in 1986 and elaborated three years later.[78,79] The clusters $[MoFe_3S_4(S_2CNR_2)_5]^{0,1-}$ (R = alkyl) were prepared. The structures of the two oxidation states, with five-coordinate iron sites and one dithiocarbamate bridging an iron and a molybdenum site, are essentially the same and are shown in Figure 4. Reaction 11 conveys the apparent assembly stoichiometry leading to the cluster monoanion. The neutral clusters are formed in a similar

$$[MoS_4]^{2-} + 3FeCl_2 + 5Na(S_2CNR_2) \rightarrow [MoFe_3S_4(S_2CNR_2)_5]^{1-} + 5NaCl + Cl^- \quad (11)$$

assembly system but require an oxidant, which has not been identified. The clusters are the only isolated examples of the $[MoFe_3S_4]^{4+,5+}$ oxidation states. It is unclear whether the formulation of $[MoFe_3S_4]^{4+}$ in Table 2 applies. Isomer shifts are not directly comparable with those of four-coordinate sites. The tendency of dithiocarbamates to stabilize higher oxidation states may bias electron distributions and diminishes the value of these clusters as analogues compared to those with thiolate ligation.

2.3.3. Properties

Single cubanes with the $[MoFe_3S_4]^{3+}$ oxidation level have an $S = 3/2$ ground state,[80,81] axial EPR spectra resembling the spectrum of FeMo-co,[71−73,76] well-resolved isotropically shifted ^1H NMR spectra,[72−74,82] and a three-member electron-transfer series involving the states $[MoFe_3S_4]^{4+/3+/2+}$. One $[MoFe_3S_4]^{2+}$ single cubane has been isolated by chemical reduction.[83] It has the same oxidation level as the reduced cluster **5** and an $S = 2$ ground state.[80]

Cluster **10** (solv = THF) binds very labile ligands at the iron and molybdenum sites, permitting an examination of relative binding affinities at the two sites.[82] Solvate clusters or ligated species involved in labile equilibrium 10 display ^1H NMR spectra consistent with trigonal symmetry. This behavior arises from solvent or ligand dissociation, chelate ring reorientation to a degenerate position roughly coplanar with a second core face, and solvent or ligand rebinding. Clusters with tightly bound ligands are not fluxional and display spectra indicative of mirror symmetry. When **10** is treated with 1−3 equiv of thiolate, binding occurs at the iron sites; the fourth equivalent binds at the molybdenum site. One equivalent of CN^- or Et_3P binds at the latter site, for which the ligand affinity order is $RS^- < Et_3P < CN^-$. The

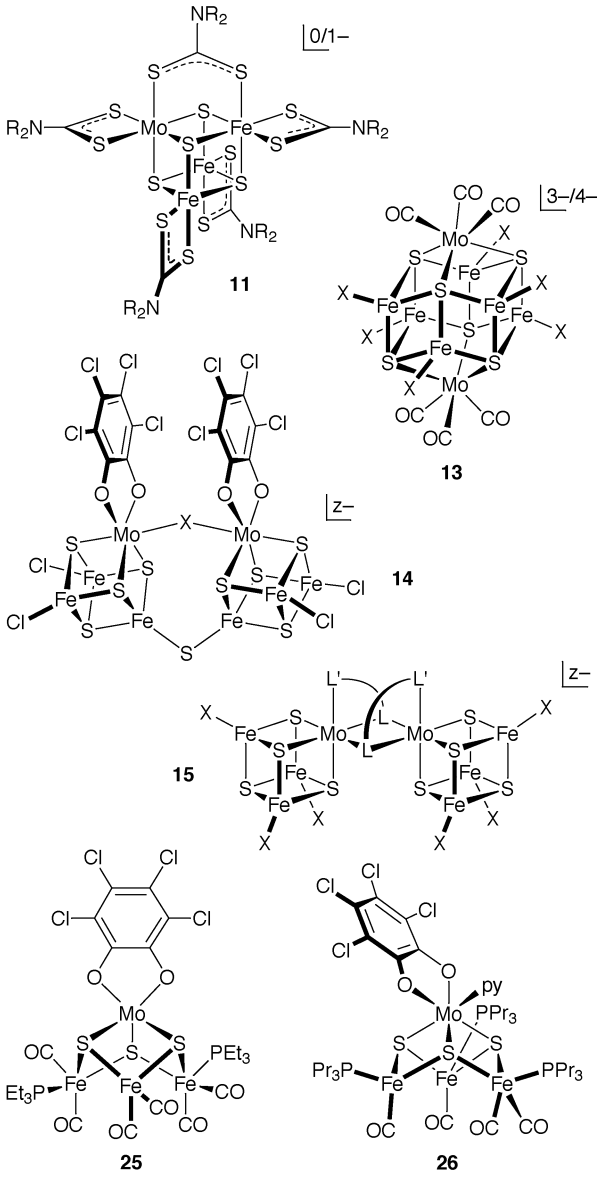

Figure 4. Clusters of note prepared in the XAS era, including the only $[MoFe_3S_4]^{4+/5+}$ clusters isolated to date (**11**), bicapped prismatic clusters (**13**), and doubly bridged double cubanes involving homometallic bridges (**14**) or bridges between molybdenum atoms only (**15**).

detection of all possible species (including isomers) in a reaction system such as $[(cat)(Et_3P)MoFe_3S_4Cl_3]^{2-}/nRS^-$ (n = 1−4) is a telling example of the sensitivity of isotropically shifted NMR spectra (^{1}H, ^{19}F) to the structures of $[MoFe_3S_4]^{3+}$ clusters.[82] Lastly, catecholate is subject to substitution by reaction with other catechols.[74] We note here a closely related reaction discovered in the next time frame. Treatment of **10** with diprotic acids such as oxalic, malic, or *N*-methylimidodiacetic acid results in substitution of catecholate in reaction 12 (Scheme 2).[84] For example, cluster **12** of proven structure has been prepared in 93% yield under the indicated conditions. This cluster is of considerable interest in the formation of another type of double cubane (section 3.3).

2.4. Other Mo–Fe–S Clusters

In the period 1985−1989, the first examples of two new cluster types were prepared; their structures are set out in Figure 4. The bicapped prismane clusters **13** (X = Cl$^-$, Br$^-$, RO$^-$) are prepared by reaction of $[Fe_6S_6L_6]^{3-}$ with excess $[Mo(CO)_3(MeCN)_3]$, which also acts as a reductant.[85−87] The prismane cluster is capped on opposite faces by $Mo(CO)_3$ groups. The cluster tetraanion can be oxidized to the trianion with ferrocenium or obtained directly by using a more nearly stoichiometric quantity of the tricarbonyl. The other new cluster type, **14**/**15**, consists of $[MoFe_3S_4]^{3+}$ double cubanes with bridging modalities different from those of **1**−**5** or **7**.[32,33] The doubly linked cluster **14** features an Fe−S−Fe bridge and variable Mo−L−Mo connectors with L = S^{2-}, OH$^-$, CN$^-$, and N_3^-.[32,88−90] Cluster **15** is doubly bridged between molybdenum atoms only. The first example, containing L−L′ = S_2^{2-},[88] was followed by clusters with mercaptoacetate, thiomalate, and thiolactate bridges.[84,89] The latter clusters are prepared by reactions analogous to **12** (Scheme 2). In all clusters, the sulfur atom is the bridge and the carboxylate a monodentate terminal ligand. Variations on **15** are Mo−L−Mo singly bridged clusters with L = N_2H_4 and pyrazine.[90] All of these bridged clusters are ultimately derived from $[(Cl_4cat)(solv)MoFe_3S_4Cl_3]^{2-}$, an example of **10** with labile ligands at the iron and molybdenum sites. Some of the double cubanes exhibit resolved redox steps for their individual clusters, exemplified by the separate reduction steps of $\{[MoFe_3S_4(SC_6H_4$-*p*-$Cl)_3]_2(\mu_2$-$S_2)_2]\}$ at −1.14 and −1.34 V in acetonitrile.[88] Cluster types **13**−**15**, while of interest in their own right, have not been further elaborated to species with compositions and structures more closely related to FeMo-co.

2.5. VFe_3S_4 Cubane Clusters

The facile synthesis of $MoFe_3S_4$ (and WFe_3S_4) clusters raised two related issues: (i) the scope of MFe_3S_4 cluster formation by self-assembly or other means, and (ii) the possible synthesis of V−Fe−S clusters, motivated by the existence of an alternative nitrogenase containing vanadium. These matters were first addressed in 1986−1987 by the reactions in Scheme 3, resulting in the formation of VFe_3S_4 single cubanes.[91−93] Highly nucleophilic $[VS_4]^{3-}$ binds 2 equiv of $FeCl_2$ to give linear cluster **16**. In key reaction 13, this cluster is reduced by $FeCl_2$ and rearranges to the cubane geometry of **17**, usually isolated as the DMF trisolvate. Reaction 13 can be

$$[VFe_2S_4Cl_4]^{3-} + 2FeCl_2 + 3solv \rightarrow [(solv)_3VFe_3S_4Cl_3]^- + [FeCl_4]^- + Cl^- \quad (13)$$

considered cluster synthesis by *fragment condensation* followed by *core rearrangement*. The fragment is $[VFe_2S_4]^+$, which appears in the product as part of the $[VFe_3S_4]^{2+}$ core. The clusters **17** (solv = MeCN)[94] and $[VFe_3S_4(S_2CNEt_2)_4]^-$ [95] were later obtained in poor yields from assembly systems in which no intermediate was isolated. The rearrangement of linear trinuclear clusters has been exploited in the synthesis of other MFe_3S_4 clusters with M = Mo/W[96−98] and Co/Ni.[99,100]

The $[VFe_3S_4]^{2+}$ core of cluster **17** and its derivatives is isoelectronic with $[MoFe_3S_4]^{3+}$ and has an $S = {}^3/_2$

Scheme 3. Synthetic Methods for $[VFe_3S_4]^{2+}$ Cubanes[a]

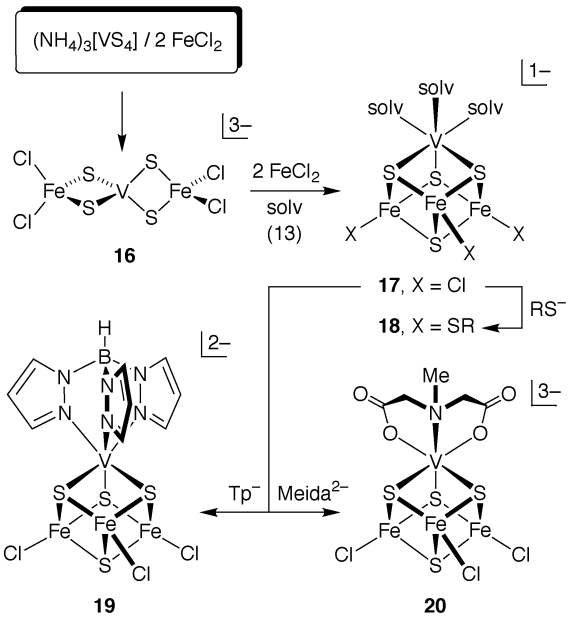

[a] Cluster **17** is the precursor to other clusters by regiospecific reactions at the iron and vanadium sites, as illustrated by the formation of **18** and **19**/**20**, respectively.

ground state.[81] The vanadium site has little affinity for thiolate, allowing ready formation of **18** (solv = DMF, Me_2SO). However, this site binds a variety of ligands, including dmpe, bpy, Tp in cluster **19**,[101] and Meida in cluster **20**.[102] Reaction of **17** (L = Me_2SO) with Na_3LS_3 affords $[(Me_2SO)_3VFe_3S_4(LS_3)]^-$, in which the core is coordinated by a trithiolate ligand designed to bind cubane clusters at the iron sites.[103] In this cluster, reactivity is directed to the vanadium site, leading to regiospecific binding of cyanide. Intermediate species in the formation of fully substituted $[(NC)_3VFe_3S_4(LS_3)]^{4-}$ are readily detected by ^{1}H NMR. Lastly, the clusters sustain a three-member electron-transfer series (Table 2), for which isomer shifts support localization of redox changes to the Fe_3S_4 fragment. In this and subsequent research, clusters containing all three oxidation states have been isolated.

2.6. Relation to Cofactor Clusters

In the search for synthetic analogues of FeMo-co and FeV-co, the single most significant result in the XAS era was the synthesis of clusters containing the MFe_3S_3 cuboidal fragment, the existence of which was proven by numerous X-ray structure determinations. Thus, the high degree of similarity of the molybdenum EXAFS of synthetic clusters and cofactor, which marked the beginning of this era,[54,55] strongly supported structure proposal **1**. When the terminal Mo−S interactions are discounted, the proposal is now known to be correct. In Figure 5 (upper), bond lengths in typical $[MoFe_3S_4]^{3+}$ [82] and $[VFe_3S_4]^{2+}$ [93] clusters are compared with crystallographic average values for FeMo-co (obtained at 1.6 Å resolution)[21] and EXAFS values for FeV-co.[38] For the most part, the agreement is quite good. The biggest discrepancies are found with the Mo−N_{His} and Mo−$O_{homocitrate}$ bond lengths. One or possibly both of the Mo−O

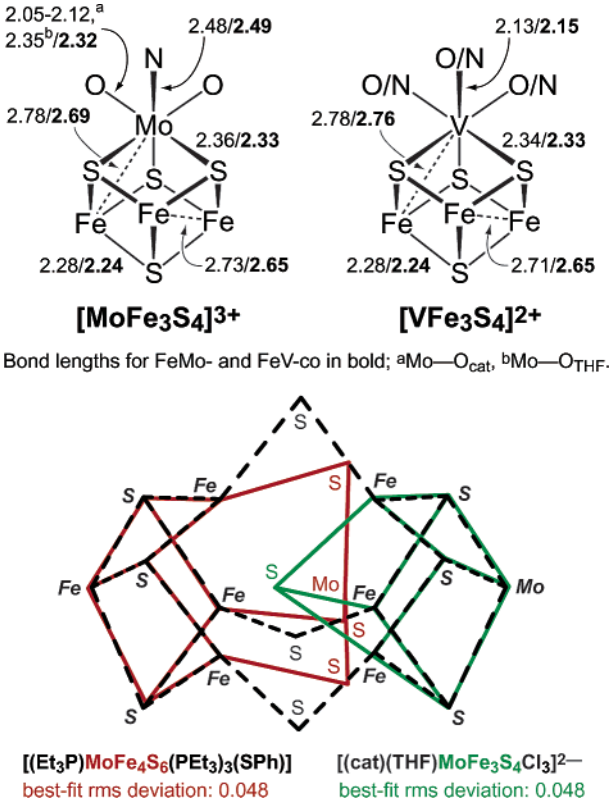

Figure 5. (Upper) Comparison of bond lengths (Å) in cubane clusters prepared in the XAS era with those in cofactor clusters (bolded values). (Left) Crystallographic values from $[(cat)(THF)MoFe_3S_4Cl_3]^{2-}$ [82] and FeMo-co in the reduced MoFe protein of *K. pneumoniae* nitrogenase (1.6 Å resolution).[21] (Right) Crystallographic values from $[(DMF)_3VFe_3S_4Cl_3]^{1-}$ [93] and EXAFS values tabulated by Eady[38] for FeV-co in the reduced MoFe protein of *A. vinelandii* nitrogenase and when extracted from the protein. Two types of Mo−O distances in analogue clusters are indicated. (Lower) Best-fit superpositions of *K. pneumoniae* FeMo-co (black dashes) with the cuboidal (Mo/Fe)-Fe_3S_3 portions of $[(cat)(THF)MoFe_3S_4Cl_3]^{2-}$ (green) and $[(Et_3P)MoFe_4S_6(PEt_3)_3(SPh)]$[109] (red). Terminal ligands have been omitted for clarity, and fitted atoms are indicated in bold italics.

bonds involve anionic oxygen and are substantially longer than the range of Mo−O_{cat} bond lengths; they agree better with the Mo−O_{THF} distance in the synthetic cluster. However, it should be noted that the apparently large differences between the crystallographically determined terminal Mo−O/N bond lengths for *Klebsiella pneumoniae* MoFe protein and those in the *A. vinelandii* MoFe protein (2.02−2.15 Å)[20] have not been explained. If this comparison had been restricted to protein EXAFS results obtained in the XAS era, the proposal that the cofactor clusters contained MFe_3S_3 fragments would still be sustained.

Certain other similarities between single cubane clusters and the native clusters were evident in the XAS era.[80,81] These included antiparallel spin coupling leading to $S = {}^3/_2$ ground states, similar EPR spectra of this state, including a slight increase in line width when substituted with ^{57}Fe and a forbidden transition at $g \approx 5.9$, and delocalized, mixed-valence structures. Then, as now, the charge distributions for the $S = {}^3/_2$ states of the analogues in Table 2 are favored as limiting descriptions.

In the XAS era, the chemistry of weak-field M−Fe−S clusters (M = Mo, V) was in its initial development period. Nearly every new cluster type and property were greeted as progressive and potentially useful in the ultimate synthesis of a cofactor cluster. Similarities in structural and electronic properties between the synthetic cubanes and cofactors were regarded by most investigators as positive indicators that synthetic efforts were moving in an appropriate direction. However, from the second-shell Fe···Fe interactions detected by EXAFS and analytical data that circumscribed the FeMo-co composition as $MoFe_{6-8}S_{7-9}$, it became evident that the native cluster was larger and thus more complex than any M−Fe−S cluster mononuclear in M = Mo or V known at the time. Consequential synthetic analogues could be identified by spectroscopic coincidence, and the true structure proven beyond doubt by its ability to reconstitute to full activity a mutant nitrogenase lacking cofactor.[36,37] Neither of these circumstances was approached. Exploratory synthesis directed at objects of unknown structure was drawing to a close. It would be revitalized by the advent of three-dimensional structural information, as the macromolecular structure era began.

3. The Macromolecular Structure Era (1992–2002)

The crystallographic analysis of the MoFe protein of *A. vinelandii* reported by Kim and Rees[23] in 1992 was the first disclosure of the three-dimensional structures of the clusters of nitrogenase. In subsequent reports by the Rees group proceeding through to the 2.0-Å resolution structure of the protein in two oxidation states in 1997,[20] the structures of FeMo-co and the P cluster have become increasingly better defined. The results of Mayer et al.[21] in 1999 established these structures in another protein at higher resolution (MoFe protein of *K. pneumoniae* at 1.6 Å). In the most recent development, Rees and co-workers[22] in 2002 located an interstitial atom in FeMo-co by a structure determination at 1.16 Å. Figure 2 conveys the most highly resolved structures of FeMo-co and the P^N cluster currently available. The initial structural report, although subject to several revisions at higher resolution, was a revelation to the biochemist attentive to the nitrogenase problem and to the inorganic chemist concerned with clusters and their synthesis. These structures were not predicted by anyone. They are the most complex metal-containing entities currently recognized in biology. In describing synthetic research directed toward these clusters, we denote the above period, starting with the first X-ray structure report and ending just before the detection of the interstitial atom, as the macromolecular structure era.

3.1. Cuboidal Fragments and Clusters

The high-nuclearity iron−sulfur clusters $[Fe_6S_6(PR_3)_4X_2]/[Fe_6S_6(PR_3)_6]^+$ (**21**, X = halide, RS^-)[104−106] and $[Fe_7S_6(PEt_3)_4Cl_3]$ (**22**)[107] are formed in assembly systems in THF with the essential components $FeCl_2$, Et_3P or Bu_3P, and $(Me_3Si)_2S$ or Li_2S. The topology of the "basket" clusters **21** and the monocapped prismane **22** have not been encountered before or since in any synthetic system lacking a tertiary phosphine. These results suggested the possibility of new Mo/V−Fe−S clusters produced by self-assembly in systems containing the foregoing components and a reactive vanadium or molybdenum source. The system in Scheme 4 was eventually developed, affording the clusters $[(Et_3P)MoFe_4S_6(PEt_3)_3Cl]$ (**23**, M = Mo, V) in modest yield.[108] Neither the core composition nor the structure of idealized trigonal symmetry had been observed previously. Both clusters **23** crystallized with imposed C_3 symmetry and are isostructural and nearly isometric. The clusters contain an Fe_4S_3 cuboidal fragment bridged by three μ_2-S atoms to a heterometal site, which exhibits unprecedented MS_3P trigonal pyramidal coordination with P−M−S = 89−90° and S−M−S = 120°. The same type of coordination applies at the three equatorial FeS_3P sites but with large angular distortions from local C_3 symmetry. The axial FeS_3Cl site, with S−Fe−S = 103° and Cl−Fe−S = 115°, has the distorted tetrahedral configuration observed in clusters such as $[Fe_4S_4(SR)_4]^{2-,3-}$.[1] The cluster core can be viewed as a monocapped derivative of a hypothetical homo- or heterometallic cluster core $M_4(\mu_2\text{-}S)_6$ of T_d symmetry. Capping of the S_3 faces generates the series M_nS_6, with n = 5−8, all of which are known.[108] The only examples with n = 5 are **23** and **24**.

The clusters **23** readily undergo substitution at the axial iron site without change in structure to yield the thiolate-substituted clusters **24** (R = Et, Ph) in 60−80% yield.[109] These clusters display well-resolved isotropically shifted spectra, the three-member electron-transfer series below whose potentials have only a small dependence on M and L = Cl^- or RS^-, and isomer shifts of the axial iron atoms suggestive of the oxidation state range $Fe^{2.75+}$−Fe^{3+} (M = V) or $Fe^{2.25+}$−$Fe^{2.5+}$ (M = Mo) in the neutral members of the series. Vanadium cluster is diamagnetic in the solid state

Scheme 4. Self-Assembly of the Clusters 23 (M = Mo, V) and Substitution of the Terminal Chloride Ligand with Thiolate To Give Clusters 24[a]

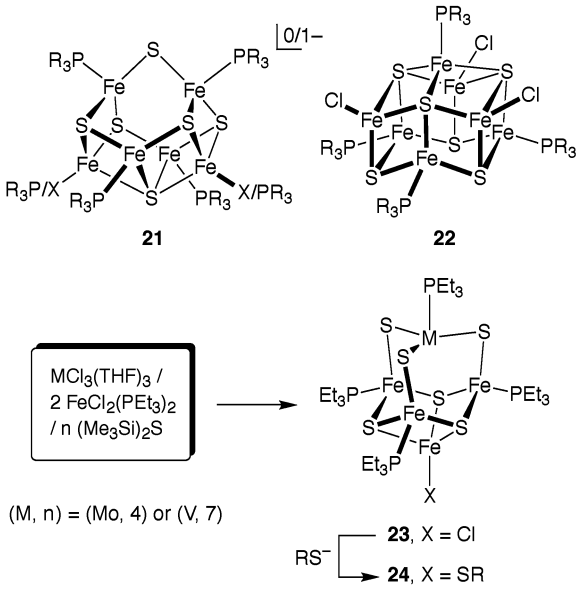

[a] Iron−sulfur clusters **21** and **22** are formed in similar assembly systems lacking the heterometal component.

at low temperature and exists in an apparent singlet−triplet equilibrium in solution; the molybdenum clusters have an $S = {}^1/_2$ or spin-admixed ${}^1/_2,{}^3/_2$ ground state. Reaction of **23** (M = V) with Li_2S results in $\{[(Et_3P)VFe_4S_6(PEt_3)_3]_2(\mu_2\text{-}S)]\}$,[102] an example of a sulfido-bridged cluster (Fe−(μ_2-S)−Fe = 134°) formed in a reaction of some generality (vide infra).

$$[(Et_3P)MFe_4S_6(PEt_3)_4L]^+ \leftrightarrow [(Et_3P)MFe_4S_6(PEt_3)_3L] \leftrightarrow [(Et_3P)M\ Fe_4S_6(PEt_3)_3L]^-$$

The first M_4S_3 cuboidal molecular cluster prepared was the venerable Roussin's black anion in the 1850s, known to have the structure $[Fe_4(\mu_3\text{-}S)_3(NO)_7]^-$ with idealized C_{3v} geometry.[110] The related clusters $[Fe_4S_3(NO)_4(PR_3)_3]^{0,+}$ have been synthesized.[111,112] These species have the same core as Roussin's anion and one phosphine bound at each equatorial iron site in a structure of overall trigonal symmetry. Coucouvanis and co-workers[113−115] have synthesized the first examples of strong-field heterometal cuboidal clusters in the form of $MoFe_3(\mu_3\text{-}S)_3$ species with carbonyls and phosphines bound at the iron sites. Examples include $[(Cl_4cat)MoFe_3S_4(PEt_3)_2(CO)_6]$ (**25**) and $[(Cl_4cat)(py)MoFe_3S_4(PPr_3)_3(CO)_4]$ (**26**) (Figure 4) and are regarded as distorted versions of the $MoFe_3S_3$ fragment of FeMo-co.[113] Bond distances in both clusters indicate an extent of direct metal−metal bonding. Core structures differ primarily by the number of bonded Fe−Fe distances. There are two in **25** (2.63, 2.70 Å) and one longer nonbonded separation (3.64 Å), whereas in **26** there are three bonded distances (mean 2.59 Å) which define a nearly equilateral triangle. The difference has been attributed to two additional valence electrons in **25**.[115] These are strong-field clusters with nonbiological ligation and indistinct oxidation states at the iron sites. However, the molybdenum atom in **26** occurs in a MoS_3O_2N coordination unit, as does this atom in FeMo-co (Figure 2). This unit is also found in the cubane **12**. The molybdenum site in $[(H_2cit)MoFe_3S_4Cl_3]^{2-}$,[84] reported as a product of reaction 12 (Scheme 2) utilizing citric acid, apparently simulates homocitrate in two of its presumed three binding interactions; an X-ray structure has not been reported. No means have yet been found of coupling together cuboidal $MoFe_3S_4$ and Fe_4S_3 units into a common cluster. The VFe_3S_3 cuboidal unit has not been separately prepared. We note that the VS_3O_2N unit in cubane cluster **20** presumably resembles vanadium coordination in FeV-co.

3.2. Structural Comparison with FeMo-co

We have observed in Figure 5 (upper) the close relationship in bond lengths between MFe_3S_3 cuboidal portions of cubane-type clusters and those in two cofactors. With the synthesis of clusters **23** and **24** in the macromolecular structure era, we can examine the correspondence between shapes of synthetic cuboidal fragments and those present in FeMo-co. In Figure 5 (lower), the least-squares superposition of cuboidal MFe_3S_3 core fragments from $[(cat)(THF)MoFe_3S_4Cl_3]^{2-}$ (green, M = Mo) and $[(Et_3P)MoFe_4S_6(PEt_3)_3(SPh)]$ (red, M = Fe) onto the corresponding subunits of FeMo-co (black dashes) is shown. As is visually apparent, the fits are excellent, with rms deviations of 0.048 Å for both comparisons. The correlation extends to the terminal donor atoms on iron (both thiolate) and molybdenum (catecholate/THF vs carboxylate/alkoxide/imidazole); these were not used in the fitting procedure, yet they show relatively modest positional deviations (0.17−0.51 Å, arising predominantly from angular variations). The similitudes are striking, especially in light of the overall geometry differences in the cluster structures as a whole. This is particularly evident for the $MoFe_4S_6$ cluster, where the μ_2-S bridges are tied to the single molybdenum atom and to phosphine-ligated trigonal pyramidal iron sites. The Fe_4S_3 fragment nonetheless maps cleanly on the cofactor structure, and this degree of geometric retention may reflect an intrinsic structural characteristic of the cluster subunit that is not understood at present. It must be noted, however, that the original macromolecular structure determinations employed small-molecule iron−sulfur clusters as models to fit the observed electron density in the protein active site, and any bias so introduced could artificially enhance the perceived structural relationship.

3.3. Sulfido-Bridged Double Cubanes

The MFe_3S_4 cubane-type clusters constitute the largest structural type of heterometal iron−sulfur clusters containing molybdenum or vanadium. They are readily prepared, and many are subject to controlled modification by ligand substitution and redox reactions. Because of their tightly bridged structures at the molybdenum sites, clusters such as **1**−**4** and **6** have not proven tractable for compositional and structural modifications directed toward cofactor clusters. This is not the case for many single cubanes with manipulable heterometal and iron sites. Taking as the initial step the preparation of *symmetrical* clusters $M_2Fe_6S_{8,9}$ compositionally related to the cofactors or P cluster, bridged double cubanes represent one potential pathway. Clearly, the *unsymmetrical* MFe_7S_9 cofactor core presents an even more formidable challenge. Sulfido-bridged double cubanes (in which sulfide is the only bridging atom) are of two types: two clusters bridged by one μ_2-S atom external to the clusters or by two μ_4-S atoms, each of which is part of a $MoFe_3S_4$ cubane core. The latter are generally referred to as *edge-bridged* (or sometimes rhomb-bridged) double cubanes. In both types, the bridge is between two iron atoms.

3.3.1. Monosulfido-Bridged Clusters

The first indications that iron−sulfur clusters could be bridged to yield double cubanes occurred in the period 1989−1990. Reaction of $[Fe_4S_4(LS_3)Cl]^{2-}$ with Li_2S gave $\{[Fe_4S_4(LS_3)]_2(\mu_2\text{-}S)]\}^{4-}$, inferred from ^1H NMR evidence.[116] Shortly thereafter, a similar reaction of $[Fe_4S_4Cl_4]^{2-}$ afforded $\{[Fe_4S_4Cl_3)]_2(\mu_2\text{-}S)]\}^{4-}$, whose bridged double-cubane arrangement was established by an X-ray structure.[117] Individual clusters are linked by an Fe−S−Fe bridge with an angle of

Scheme 5. Synthesis of Sulfido- and Oxo-Bridged Double Cubanes 28−30 by Cluster Coupling Reactions Based on Single Cubanes 12 and 27

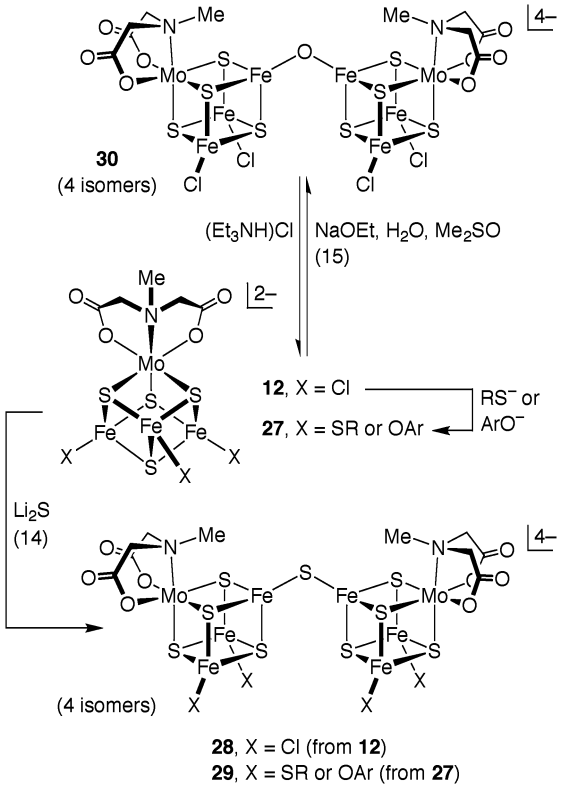

102.2°. These results prompted a synthetic approach to FeMo-co that is summarized in Scheme 5.[102,118] All clusters are in the $[MoFe_3S_4]^{3+}$ oxidation state.

The molybdenum site in single cubane **12** is coordinated by the facial tridentate ligand Meida, protecting the site from further reaction and directing ligand substitution to the iron sites. The clusters **27** are easily accessible by ligand substitution at the iron sites. The key reaction in the scheme is coupling of two cubanes through a sulfido bridge, as in reaction 14. Clusters **28** and **29** have been isolated, but

$$2[(\text{Meida})MoFe_3S_4Cl_3]^{2-} + Li_2S \rightarrow \{[(\text{Meida})MoFe_3S_4Cl_2]_2(\mu_2\text{-}S)\}^{4-} + 2LiCl \quad (14)$$

diffraction-quality crystals have not been obtained, possibly because the clusters are obtained as a mixture of isomers, as indicated by ^{1}H NMR spectra.[102] Four isomers are possible because of the different ways of bridging individual cubanes with C_s symmetry. These clusters have been securely identified by a combination of NMR, electrospray mass spectrometry, and voltammetry, which reveals coupled redox processes. For example, **28** in DMF displays two reductions at −1.01 and −1.34 V. The premise underlying this approach is that removal of terminal ligands of a bridged double cubane generates the $[Mo_2Fe_6S_9]^{4+}$ core, which has the same total metal and sulfide content as FeMo-co. The deligated cluster might then undergo a skeletal rearrangement to a stable product which could have the topology of FeMo-co. In that event, the product would contain two isomers. This approach was conceived about six years prior to the identification of an interstitial atom in FeMo-co, when the six iron sites bridged by μ_2-S atoms were thought to have unorthodox three-coordination. A related development in the course of this work was reaction 15, affording the oxo-bridged cluster **30**. While this approach to FeMo-co is compromised by the absence of an interstitial atom, it did provide entry to the previously unknown chemistry of monosulfido- and monooxo-bridged heterometal double cubanes. Whether such clusters will ultimately be of use in cofactor synthesis remains to be seen.

$$2[(\text{Meida})MoFe_3S_4Cl_3]^{2-} + 2NaOEt + H_2O \rightarrow \{[(\text{Meida})MoFe_3S_4L_2]_2(\mu_2\text{-}O)\}^{4-} + 2NaCl + 2EtOH \quad (15)$$

3.3.2. Edge-Bridged Double Cubanes

The first example of an edge-bridged double cubane is cluster **31**, prepared as indicated in Scheme 6 by Demadis et al.[119] in 1995. The reaction results in core reduction of **10**; the product contains two $[MoFe_3S_4]^{2+}$ units. While the reaction stoichiometry is obscure, the reductant doubtless is the phosphine, which is oxidized to Et_3PS. Phosphine as a reductant in the synthesis of related clusters has been demonstrated in, e.g., the conversion of $[Fe_4S_4Cl_4]^{2-}$ to $[Fe_4S_4(PPr^i_3)_4]^+$ and **10** to $[(Cl_4cat)(MeCN)MoFe_3S_4(PPr^i_3)_3]$, where the phosphine sulfide was directly detected.[120] Edge-bridged double cubanes have actual or idealized centrosymmetry, which places the heterometal atoms and the monodentate ligand at the molybdenum site in **31** and similar clusters in transoid positions. The two cubanes are linked by a planar $Fe_2(\mu_4\text{-}S)_2$ rhomb, with the Fe−(μ_4-S) bond between cubanes shorter than that within them. In the triclinic modification of **31**, for example, the metric parameters of the rhomb are Fe−S = 2.367 and 2.245 Å, Fe−Fe = 2.639 Å, Fe−S−Fe = 69.7°, and S−Fe−S = 110.3°.[120] While examples are not numerous, the Fe_2S_2 rhombic bridge has been found only in *reduced* clusters ($[Fe_4S_4]^{+,0}$, $[MoFe_3S_4]^{2+,+}$, $[VFe_3S_4]^+$), where the nucleophilicity of a core sulfide atom is sufficient to sustain four bridging interactions. This is the case in edge-bridged clusters with Fe_8S_8,[121,122] $V_2Fe_6S_8$,[123] and $Mo_2Fe_6S_8$[120,124,125] cores. Clusters of this structure type have proven to be highly reactive. They are precursors to two significant groups of clusters: those containing the $MoFe_3S_3$ cuboidal unit, such as **25** and **26**,[113−115] and others which replicate the topology of the P^N cluster of nitrogenase.

3.4. Topological Analogues of P-Clusters

The P^N cluster of nitrogenase, with its Fe_6S_9 core containing three types of Fe−S−Fe bridging interactions, is currently the most complex iron−sulfur cluster of known structure in biology. As such, it presents a substantial challenge to the synthetic analogue approach. Its preparation would be valuable not only from the synthetic perspective but also because it would potentially allow examination of structural and electronic features that are dependent on oxidation level. The X-ray structure of a cofactor-

Scheme 6. Reactions Affording Edge-Bridged Double Cubane 31, Higher-Nuclearity Clusters 32 and 33 Containing $Mo_2Fe_6S_9$ Fragments with the Structure of the P^N Cluster of Nitrogenase, and Cluster 34 Containing an Unusual $Mo_2Fe_6S_8$ Core Motif

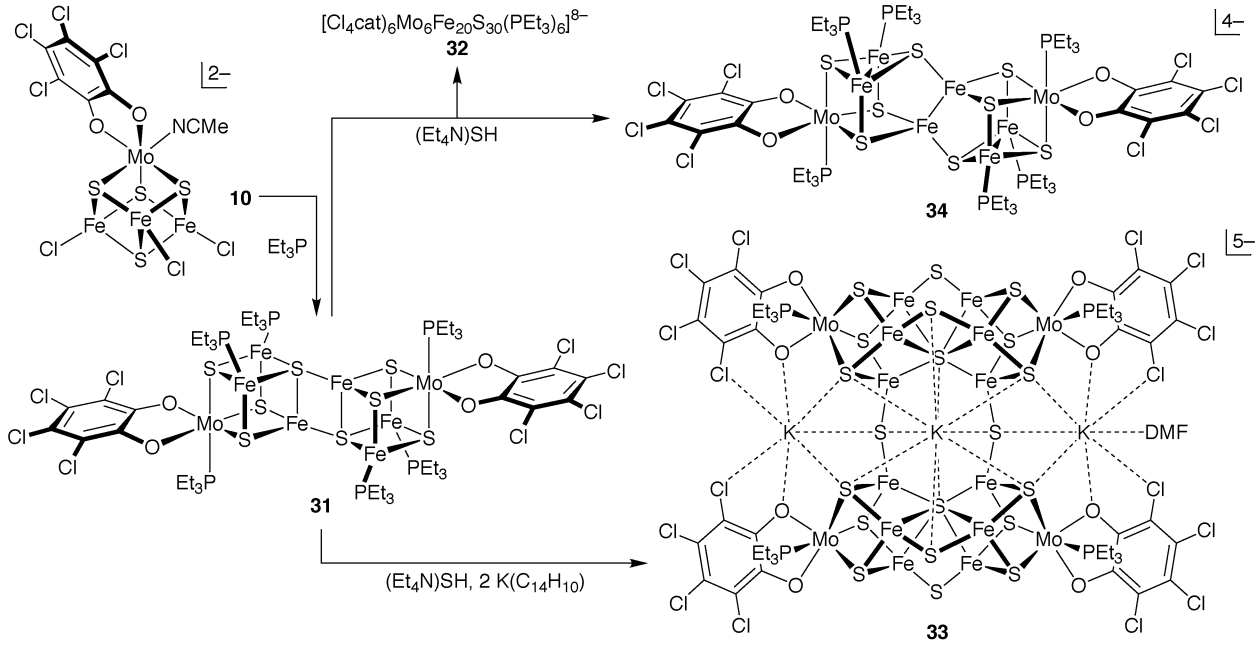

less mutant of the *A. vinelandii* MoFe protein containing P^N clusters has been reported.[126] Summarized in Scheme 6 are reactions directed toward products with the P^N -cluster structure and based on edge-bridged double cubane **31**. The reactions involve the common reagent $(Et_4N)SH$ but under rather specific conditions of reaction stoichiometry and solvent, and of solvent and cations for purification by crystallization. Full details are found in the references cited.

3.4.1. Higher Nuclearity Clusters

Treatment of **31** with 2 equiv of hydrosulfide, followed by removal of volatile components, extraction of the residue with NMF, and recrystallization as a mixed Et_4N^+/Bu_4N^+ salt, afforded the high-nuclearity cluster **32**.[127] The cluster structure (not shown) is complicated. However, two different fragments are discernible: $Mo_2Fe_8S_{12}$, located at the center of the cluster, and two $Mo_2Fe_6S_9$ units, linked to the central fragment by Fe−S−Fe bridges. The fragments contain octahedral $(Cl_4cat)(Et_3P)Mo(\mu_3\text{-}S)_3$ and tetrahedral FeS_4 coordination units in which all sulfide ligands are bridging. The smaller fragments have idealized C_s symmetry and the bridging pattern $Mo_2Fe_6(\mu_2\text{-}S)_2(\mu_3\text{-}S)_6(\mu_6\text{-}S)$; two $MoFe_3S_4$ cubane-type units are linked by a μ_6-S and two μ_2-S bridges. This is the arrangement in the P^N cluster, with two molybdenum atoms replacing two iron atoms and two μ_2-S atoms simulating two $\mu_2\text{-}S_{Cys}$ atoms. Thus, the $Mo_2Fe_6S_9$ fragments provide the first demonstration that the P^N topology can be achieved in a synthetic cluster. However, the question remained as to whether the structure of these fragments was enabled by the cluster structure in its entirety. Further, the properties of the fragments could not be disentangled from those of the whole cluster. For example, the isomer shift of 0.52 mm/s is consistent with a mean oxidation state $Fe^{2.4+}$,[127] but does not directly reflect the charge distribution within the fragment of interest. A net charge cannot be assigned to this fragment. Likewise, all of the six redox steps between −0.44 and −1.76 V in acetonitrile[125] are likely to be properties of the entire cluster.

In an attempt to attain the P^N-cluster topology in a less complicated environment, the reaction system **31**/2$(Et_4N)(SH)$/2$K(C_{14}H_{10})$ in THF was investigated. After cation metathesis, the high-nuclearity cluster $[(Cl_4cat)_4(Et_3P)_2Mo_4Fe_{12}S_{20}K_3(DMF)]^{5-}$ (**33**) was isolated as the Ph_3PMe^+ salt, which was identified crystallographically.[125] The structure of **33** consists of two isostructural $Mo_2Fe_6S_9$ fragments of idealized C_s symmetry connected by two Fe−$(\mu_2$-S)−Fe bridges. In addition, three potassium ions are intercalated between the clusters and interact with them to give the cluster additional stability. The fragments consist of $MoFe_3(\mu_3\text{-}S)_3$ cuboidal units bridged by a common μ_6-S atom and containing octahedral MoO_2PS_3 and tetrahedral FeS_4 coordination units. These fragments are isostructural with two such fragments present in the more complex cluster **32**. Based on overall shape, atom connectivities, and metric parameters, the two $[Mo_2Fe_6S_9]^{2+}$ fragments in **33** are topological analogues of the P^N cluster. The isomer shift of 0.52 mm/s (4.2 K) is the same as that for **32**. The synthetic procedure achieved the goal of producing a cluster of lower nuclearity than **32** containing $Mo_2Fe_6S_9$ fragment(s). Also obtained from reaction of **31** with hydrosulfide under reducing conditions was cluster **34**, a minor product obtained in a mixed crystal with the Et_4N^+ salt of the monoanion of **31**.[125] The latter has been prepared independently, but **34** has not. The cluster is included here because its core structure, with an Fe−Fe bond of 2.41 Å, presents a structural motif not found elsewhere. While the future utility of **34** depends on an independent synthesis, we note a potential reaction of interest:

Scheme 7. Synthetic Pathway to the Molybdenum-Containing P^N-Cluster Topological Analogue 40

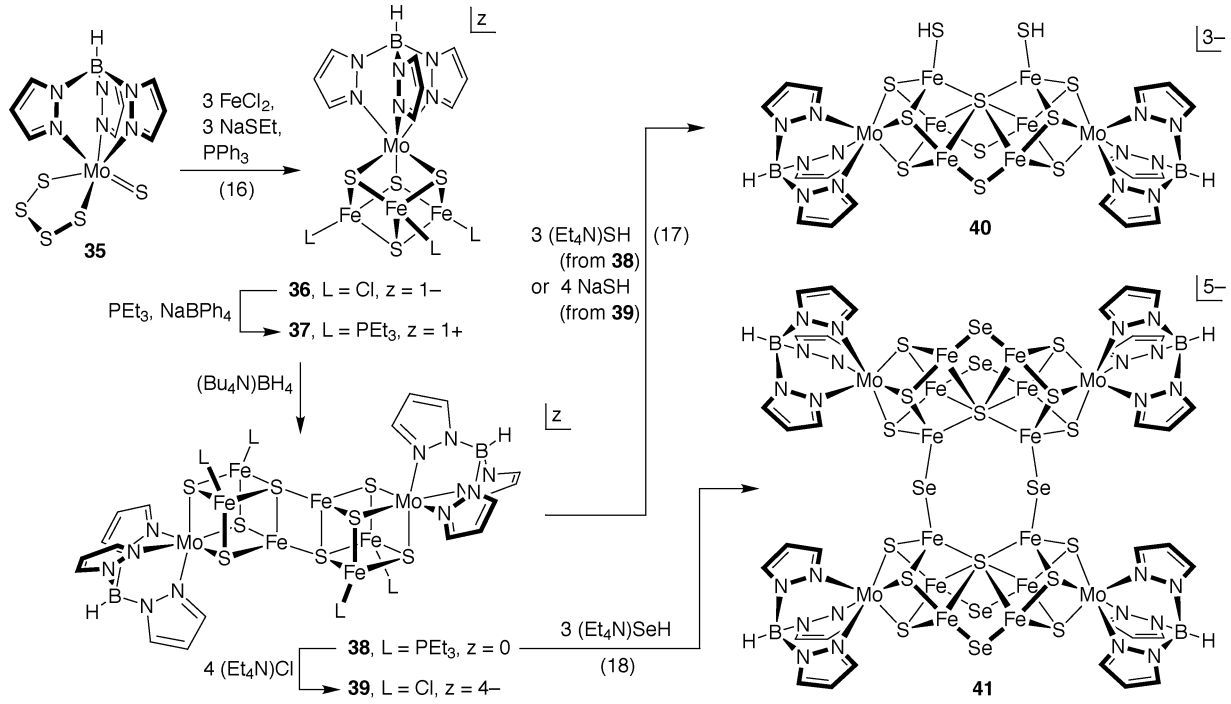

oxidative addition of sulfur into the Fe−Fe bond to produce a $[Mo_2Fe_6S_9]^0$ species that is more reduced than the core portions of **33**.

3.4.2. Molecular Clusters with P^N-Cluster Topology

Synthesis and Structures. While cluster **33** is an appreciable simplification over **32**, it is not the desired single P-cluster analogue free of perturbing bridging interactions. A route to such a cluster has been devised and is presented in Scheme 7.[128,129] It is again based on the reactivity of an edge-bridged double cubane, but one in which the molybdenum sites are trigonally symmetric in order to avoid isomeric product mixtures. The scheme begins with self-assembly reaction 16, utilizing Mo^{IV} complex **35**,[130] whose tetrasulfide ring is subject to reduction to afford sulfide. The reaction yields **36**,[131] the first

$$2[(Tp)MoS(S_4)]^- + 6FeCl_2 + 6NaSEt + 2PPh_3 \rightarrow 2[(Tp)MoFe_3S_4Cl_3]^- + 3EtSSEt + 2Ph_3PS + 6NaCl \quad (16)$$

trigonally symmetric $MoFe_3S_4$ single cubane to have been prepared (excluding **6**). By reductive substitution, **36** is converted to **37**, which is reduced by borohydride to the neutral double cubane **38**. This is the first cluster isolated in the all-ferrous $[MoFe_3S_4]^+$ oxidation state (Table 2). Substitution of **38** with chloride gives **39**. Treatment of **38** with 3 equiv of hydrosulfide in reaction 17 results in the formation

$$[(Tp)_2Mo_2Fe_6S_8(PEt_3)_4] + 3HS^- \rightarrow [(Tp)_2Mo_2Fe_6S_9(SH)_2]^{3-} + 4PEt_3 + {}^1/_2H_2 \quad (17)$$

of a new cluster **40**, isolated in 86% yield as the black crystalline Et_4N^+salt. One-half equivalent of dihydrogen is proposed but not established to account for the $[Mo_2Fe_6S_9]^+$ core oxidation level, which is one electron more oxidized than $2[MFe_3S_4]^+ + S^{2-}$. In a related method, double cubane **39** with 4 equiv of NaSH in acetonitrile gives **40** in 82% yield as the Et_4N^+salt.

The structure of cluster **40** is shown in Figure 6 (upper). Reaction 17 proceeds with displacement of the phosphine ligands, substantial core rearrangement with incorporation of one additional sulfide atom, and binding of two terminal hydrosulfide ligands. Comparison with Figure 2 demonstrates a close topological relationship between the P^N cluster and **40**, which consists of two $MoFe_3(\mu_3\text{-}S)_3$ cuboidal fragments linked by two μ_2-S atoms, simulating two μ_2-S_{Cys} bridges and one μ_6-S atom. The core bridging pattern is $[Mo_2Fe_6(\mu_2\text{-}S)_2(\mu_3\text{-}S)_6(\mu_6\text{-}S)]^+$. Each iron atom has distorted tetrahedral FeS_4 coordination in a structure with idealized C_{2v} symmetry. Fragments of the precursor cluster **38** are evident as two (Tp)-$MoFe_3S_3$ portions of **40** (e.g., Mo(1)Fe(1−3)S(1−3)), within which dimensional changes are small. The molybdenum atoms retain distorted octahedral coordination, and mean Mo−N, Mo−S, and Mo−Fe distances change by ≲0.04 Å. The major structural changes in the **38** → **40** conversion are the deconstruction of the bridging rhomb, formation of two bridges centered at μ_2-S(7,9), and creation of six bridges centered at μ_6-S(8) between the Fe_3 faces of two cuboidal fragments. The dimensions of the μ_2 bridges are normal, the mean values of Fe−S−Fe angles and Fe−S distances being 75.0° and 2.224 Å, respectively. Other bond distances are not exceptional, and the Fe−S bond lengths, unlike those of **38**, adhere to the order Fe−(μ_2-S) < Fe−(μ_3-S) < Fe−(μ_4-S).

With two $MoFe_3S_4$ cubanes present in **38**, a reasonable supposition is that the μ_6-S atom introduced in reaction 17 originates in the external hydrosulfide

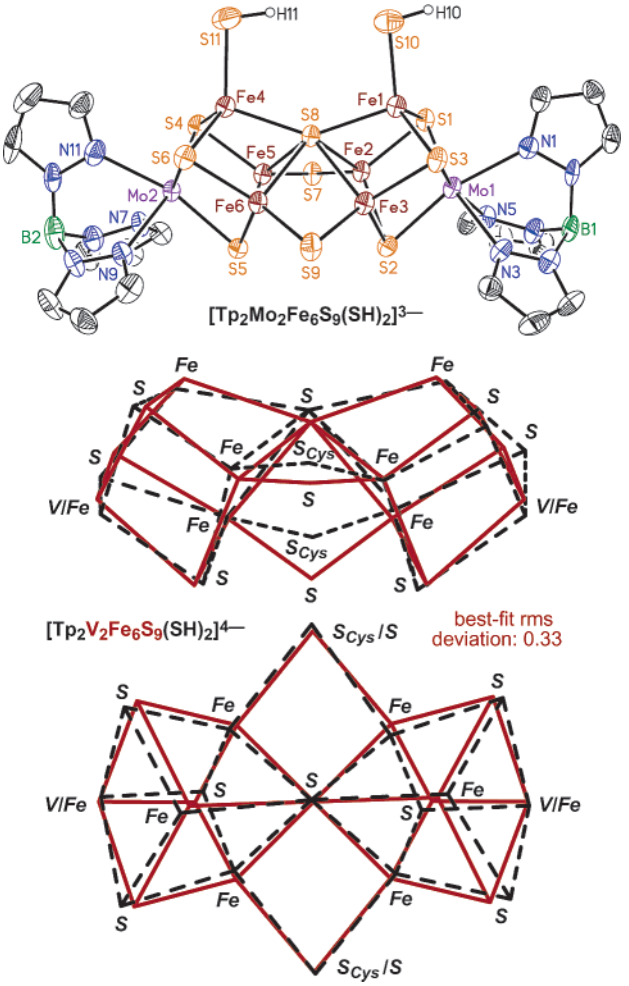

Figure 6. (Upper) Structure of $[Tp_2Mo_2Fe_6S_9(SH)_2]^{3-}$ (**40**) showing 50% probability ellipsoids; $[Tp_2V_2Fe_6S_9(SH)_2]^{4-}$ (**44**) is isostructural. (Middle and lower) Best-fit superposition (two orientations) of the P^N cluster of nitrogenase (*K. pneumoniae* MoFe protein, 1.6 Å resolution)[21] and the $[V_2Fe_6S_9]^0$ core of cluster **44**.

reactant. However, this does not appear to be the case. Using selenide as a surrogate for sulfide, reaction 18 was carried out.[129] Product cluster **41**

$$2[(Tp)_2Mo_2Fe_6S_8(PEt_3)_4] + 6HSe^- \rightarrow [(Tp)_4Mo_4Fe_{12}S_{14.5}Se_{5.5}]^{5-} + 8PEt_3 + {}^3/_2H_2 + H_2S + {}^1/_2HS^-/HSe^- \quad (18)$$

consists of two fragments $[(Tp)_2Mo_2Fe_6S_9]^{0,-}$, doubly bridged by μ_2-Q (Q = S, Se) and related by a two-fold axis. The bridge atoms occupy the positions of the hydrosulfide ligands in **40**. Cluster composition was obtained by elemental analysis, and the position of the selenium atoms was determined by X-ray structure refinement. Dominant occupancy of selenium atoms (≳90%) occurs at the doubly bridging positions internal and external to the cluster core, as indicated in **41**, and full occupancy by sulfur atoms at other positions. It is, therefore, probable that the μ_6-S atom derives from the core of precursor **38** rather than from external sulfide.

To determine if the P-cluster structure could be stabilized in other molecules, Scheme 8 was pursued.[128,132] This procedure parallels closely Scheme

Scheme 8. Synthetic Pathway to the Vanadium-Containing P^N-Cluster Topological Analogue 44

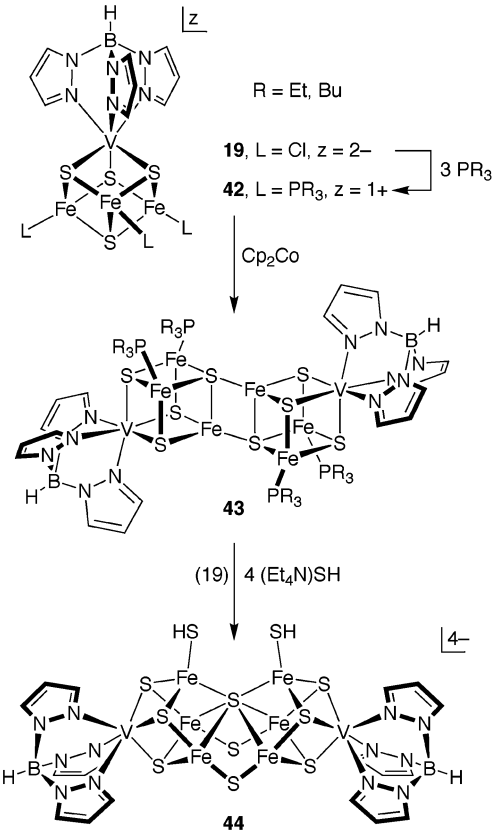

7. The initial step of phosphine substitution occurs without reduction to afford **42**. Reduction of the cluster with cobaltocene yields double cubane **43**, isostructural (R = Et) with **38** and one of only two clusters thus far isolated in the all-ferrous $[VFe_3S_4]^+$ oxidation state.[123] Reaction 19 leads to cluster **44**, obtained in ca. 50% yield as the Et_4N^+ salt. Clusters

$$[(Tp)_2V_2Fe_6S_8(PEt_3)_4] + 4HS^- \rightarrow [(Tp)_2V_2Fe_6S_9(SH)_2]^{4-} + H_2S + 4PEt_3 \quad (19)$$

40 and **44** are isostructural and nearly isoelectronic (112 vs 113 valence electrons). The cluster has a crystallographically imposed two-fold axis which contains atom μ_6-S and is perpendicular to the Fe_4 plane in the center of the molecule.

The μ_6-S atom and its associated interactions constitute the most extraordinary part of the structures of **40** and **44**. Sextuply-bridging sulfur atoms are not unprecedented in synthetic clusters, but they are rarely encountered. The Fe−(μ_6-S)−Fe angles of 141.0° in **40** and 140.8° in **44** are identical and are the largest Fe−S−Fe bond angles in the structures. This angle is 135.3° in **32** and 138.9° in **33**. Detailed descriptions of the structures of **40** and **44** are available elsewhere.[129,132] Comparison of the cores of these clusters with the $Mo_2Fe_6S_9$ fragments of **32**[127] and **33**[125] leaves no doubt that the former are isostructural molecular versions of these fragments. Clusters **40** and **44** have the same overall shape as the P^N cluster. A best-fit superposition of the $V_2Fe_6S_9$

core of **44** with the core atoms of the native cluster, shown in Figure 6 (lower), leads to an rms deviation of 0.33 Å in atom positions. The corresponding deviation for **40** is 0.38 Å, and for **33** it is 0.26 Å. One source of the deviation between synthetic clusters and the P^N cluster is the significantly larger Fe−(μ_6-S)−Fe angle of 158° and its attendant effect on atom positions in the native cluster. The differences of a Mo_2Fe_6 or a V_2Fe_6 instead of an Fe_8 metal content and two μ_2-S atoms instead of two μ_2-S_{Cys} bridges notwithstanding, we conclude that cluster **40** and **44** are the initial examples of *molecular* topological analogues of the P^N cluster of nitrogenase.

Properties. The trigonally symmetric terminal ligand at the heterometal site has two functions. Like the Meida ligand in **12** (Scheme 5), it is a protecting group, directing reactions to other metal sites. It does not allow geometric isomers, a property that may be responsible for the ability to isolate all of the compounds in Schemes 7 and 8 in crystalline form. Tridentate ligands L−L′−L at heterometal sites can potentially generate two diastereomers with the P^N-cluster topology. In acetonitrile solution, clusters **40** and **44** exhibit ^{1}H NMR spectra containing two sets of isotropically shifted pyrazolyl proton signals in an intensity ratio of 2:1, consistent with the solid-state structure. The Mössbauer spectrum of **40** at 4.2 K consists of a broadened quadrupole doublet with isomer shift $\delta = 0.55$ mm/s.[129] The spectrum of **44** at the same temperature shows two quadrupole doublets with 2:1 intensity ratio and $\delta = 0.52$ (2) and 0.59 (1) mm/s ($\delta_{av} = 0.54$ mm/s).[132] The empirical relationship between isomer shift and oxidation state (Table 2) gives $s \approx 2.3$, indicating that the clusters are substantially reduced. The Fe−SH bond length of 2.327(3) Å in **44** is practically the same as that in $[(Tp)VFe_3S_4(SH)_3]^{3-}$ (2.345(1) Å) and longer than that in $[(Tp)VFe_3S_4(SH)_3]^{2-}$ (2.297(1) Å).[132] The mean Fe−SH bond length in **40** (2.288(11) Å) and its lesser charge suggest a more oxidized set of iron atoms. The formulations $[V^{3+}{}_2Fe^{2+}{}_6S_9]^0$ and $[Mo^{3+}{}_2Fe^{2+}{}_5Fe^{3+}S_9]^+$ are currently favored as the limiting charge descriptions of **44** and **40**, respectively. They retain the heterometal oxidation states assigned to single cubanes (Table 2). One implication of these descriptions is that both clusters should be susceptible to oxidation. Indeed, **40** shows three oxidation steps at $E_{1/2} = -1.09$, -0.71, and -0.43 V in acetonitrile.[129] Cluster **44** does not show well-defined redox behavior. Derivatives of these clusters should be useful in further elucidation of properties. As will be seen, an all-iron (Fe_8S_9) species with the P^N-cluster topology has been prepared in the next research time frame (Section 4.2.3).

4. The Interstitial Atom Era

The recent revelation of an interstitial monatomic ligand at the heart of FeMo-co[22] was made possible only with the attainment of high-resolution macromolecular diffraction data, and it could therefore be viewed as just the latest culminating achievement in the continuing, long-term effort aimed at a comprehensive structural description of the nitrogenase proteins. The significance of this finding, however, is not so easily dismissed. For the past decade, all inquiry and speculation concerning biological nitrogen fixation have been guided by an overarching macromolecular visualization of FeMo-co, whose most striking and startling aspect was the occurrence of six three-coordinate, somewhat inwardly pyramidalized iron centers surrounding a small empty volume at the center of the cluster. The addition of the new core ligand fills this void, normalizes the formerly anomalous iron geometries, and generally rewrites molecular conceptions of the subject. The varied ramifications of this discovery mark it, from both chemical and biological standpoints, as the third defining event in the structural elucidation of the nitrogenase clusters.

At present, the existence of this central atom depends entirely on the results of a single high-resolution crystallographic study;[22] indeed, the interstitial component is notable for having escaped all other forms of physical and chemical detection. Conclusive proof of its reality thus awaits independent positive confirmation, preferably by techniques complementary to macromolecular crystallography. The precise identity of this core ligand is less certain still: bond distances and resolution-dependent electron density profiles from the structural analysis suggest a light (2p) element best described as nitrogen. Property predictions derived from density functional calculations[133−135] support this assignment and illustrate the growing potential for modern computational methods to guide experiment in transition metal chemistry.[136] A very recent ENDOR/ESEEM investigation concludes (from negative evidence) that the newly found ligand is not nitride arising from enzymatic reduction of dinitrogen substrate.[137] Notwithstanding its provisional status, the interstitial ligand is intuitively satisfying from the perspective of known structural inorganic chemistry, and we will accept both its existence and its qualified identity—nitride, for want of a better candidate—in the remainder of this review.

The revision of the FeMo-co model elevates the challenge of the analogue problem. The methodological inroads made when FeMo-co was viewed only as a high-nuclearity, heterometallic Mo−Fe−S cluster must now be adjusted to accommodate the presence of an unprecedented non-sulfide core ligand, deeply embedded in, and apparently integral to, the cluster framework. At the time of this writing, the finding of the interstitial atom is still too fresh and its nature too novel to have yielded (to our knowledge) any direct synthetic response. Nevertheless, we present below some observations on potentially relevant synthetic chemistry.

4.1. Cluster Nitrides

The existent chemistry of cluster-bound nitride (defined here as μ_n-N^{3-} ligation with $n \geq 3$) provides one logical starting point for synthetic consideration. We have recently surveyed the structural consequences of this ligand motif, the details of which are available in a separate account.[35] There exist ca. 100 structurally characterized complexes of cluster-bound nitrides, evenly distributed among bridging orders

ranging from μ_3 to μ_6. These nitride-containing clusters belong to three distinct categories: (i) mid-to-high-valent early transition metal clusters (Groups 4−6), which describe all complexes containing μ_3-nitrides, as well as a few isolated examples with higher bridging orders; (ii) low-valent middle-to-late transition metal carbonyl clusters (mainly Groups 8−9, but also heterometallic species containing these elements plus Group 6−10 metals in their cores), in which almost all nitrides of higher bridging orders (μ_{4-6}) are found; and (iii) Au(I) phosphine clusters, which form a limited set of μ_4- and μ_5-nitride compounds that are set apart by the structural effects of aurophilic bonding. Interstitial bridging (where the ligand resides completely inside its metal coordination polyhedron) exists in all type (iii) cluster nitrides, but is restricted to μ_5 (sometimes) and μ_6 (always) modes for transition metal systems.

The preparative routes to cluster-bound nitrides mirror the divisions in compound classes. For type (i) and type (iii) clusters, the nitride ligand is most often incorporated through simple acid/base (or nucleophile/electrophile) chemistry using a fully reduced nitrogen source—typically ammonolysis,[138] although N-desilylation[139] is also employed. The other principal tactic for nitride synthesis involves reduction of an oxidized nitrogen precursor, via either a reduced metal center or a reduced co-ligand; the reaction of azide with a low-valent metal complex, widely applied to introduce terminal nitride ligation in mononuclear species, exemplifies this approach.[140] The preparation of type (ii) carbonyl nitride clusters relies exclusively on this second method, either through metal-induced deoxygenation of NO (either preligated or delivered externally via NO or NO^+) by CO to give CO_2 and nitride[141] or, infrequently, via azide addition to bound CO to give ligated isocyanate and N_2, followed by CO de-insertion.[142] Finally, in addition to these primary synthetic entryways, high-nuclearity nitride clusters have also been obtained with some frequency through secondary paths, by capping, condensing, or otherwise derivatizing preexisting nitride complexes. Other avenues leading to molecular metal nitrides (generally noncluster cases) have been summarized elsewhere.[140]

As a weak-field, exchange-labile, redox-active iron−sulfur system, FeMo-co lies well outside the three observed classes of nitride-containing clusters; the putative nitride environment in FeMo-co is therefore singular and does not appear closely related to existing nitride chemistry. At this juncture, it is not clear which aspects of known nitride synthesis chemistry can be adapted to established methods for the construction and manipulation of iron−sulfur clusters, but it does seem certain that further development in fundamental aspects of inorganic synthesis will be prerequisite to the subsequent pursuit of FeMo-co analogues.

4.2. Iron Clusters with Other Nitrogen Anions

Although nitride ligation is currently unknown in weak-field iron clusters, there does exist an emerging chemistry that involves the substitutionally related imide (RN^{2-}) and amide (R_2N^-) ligands. The development of this chemistry was inspired, in part, by mechanistic conjectures that followed the first nitrogenase protein structures. Two observations fueled the speculation: (1) the (original) crystallographic visualization of multiple three-coordinate, ostensibly unsaturated iron centers within FeMo-co provided plausible sites for substrate binding; and (2) the (probable) existence of a variant nitrogenase containing only iron[5,6,39] demonstrated that a heterometal was not an absolute requirement for activity. These considerations, among other views, led to the proposition that dinitrogen binding and reduction were effected through bridging interactions at the anomalous central iron sites in FeMo-co. The notion of iron−sulfur clusters with nitrogen core ligands, as posited and extrapolated from these mechanisms, and the complete absence of any corresponding synthetic precedent prompted one of us (S.C.L.) to investigate iron−nitrogen interactions in broadly similar environments. The present discovery of the interstitial ligand within FeMo-co removes the structural basis for these proposals and leaves their status uncertain. Nevertheless, the chemistry of these nitrogen anions, the physical and chemical properties of which partially resemble those of nitride, may provide a useful methodological foundation for further investigation. Selected examples emphasizing synthesis and reactivity are provided here.

Scheme 9. Synthesis of the All-Ferric Imidothiolate Cubane Cluster 47 by Self-Assembly (Ar′ = 2,6-Disubstituted Phenyl)

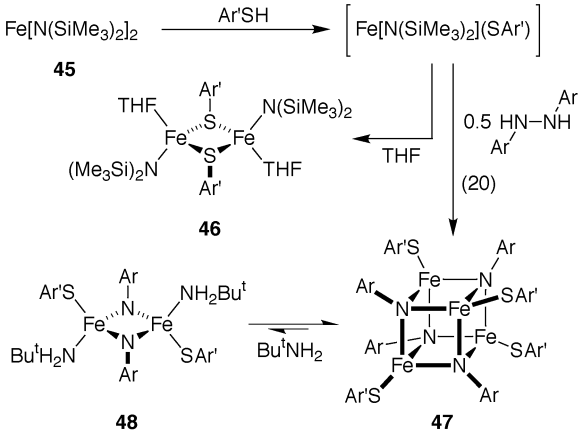

4.2.1. Imidoiron Clusters: Synthesis

Weak-field iron−imide clusters were first obtained from reaction systems designed to mediate N−N bond reduction.[143] As outlined in Scheme 9, the synthesis originates from ferrous bis(amide) **45**, with the bis(trimethylsilyl)amide ligand providing steric control of the labile high-spin metal environment and serving as a strong latent base for protonolysis chemistry. Treatment with 1 equiv of moderately hindered arylthiol allows the selective metathesis of amide for thiolate without disproportionation; heteroleptic diferrous complex **46** can be isolated when this reaction is conducted in THF. Further reaction with 0.5 equiv of 1,2-diarylhydrazine leads to the formation of neutral cubane cluster **47**, the first example of a weak-field imidoiron cluster. The cluster assembly

Scheme 10. Synthesis of Imidochloro Cubane Clusters 49 (Main Product), 50, and 51 with a Terminal Imido Ligand by Self-Assembly, and Cuboidal Cluster 54 by Fragment Condensation of 52 and 53

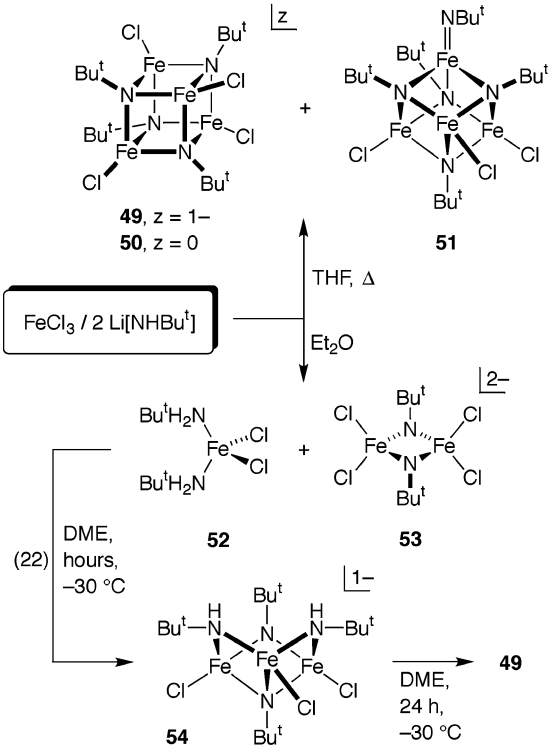

sequence is stoichiometrically exact and formally couples the two-electron reduction of the diarylhydrazine to the one-electron oxidation of Fe^{II} to Fe^{III} (reaction 20). In the presence of excess alkylamine,

$$4[Fe(N(SiMe_3)_2)_2] + 4Ar'SH + 2ArNHNHAr \rightarrow [Fe_4(\mu_3\text{-}NAr)_4(SAr')_4] + 8HN(SiMe_3)_2 \quad (20)$$

the tetranuclear cubane cluster disassembles into amine-capped dinuclear component clusters **48**; this process is reversible, with evaporation of a solution containing excess amine and the dinuclear cluster resulting in fragment condensation and recovery of the cubane cluster.[144]

The recognition of the all-ferric imide cluster **47** led to attempts to access imidoiron clusters directly from fully reduced imide sources, without intervening redox chemistry. Equation 21 presents one balanced reaction, involving a coupled anion metathesis/proton transfer using two simple reagents (ferric chloride and a reactive, soluble lithium organoamide), that

$$4FeCl_3 + 8Li(NHBu^t) \rightarrow [Fe_4(\mu_3\text{-}NBu^t)_4Cl_4] + 4Bu^tNH_2 + 8LiCl \quad (21)$$

leads, in theory, to an imidoiron(III) cubane. In practice, the outcome of this reaction is complex and condition-dependent. Two limiting experimental cases are summarized in Scheme 10. When the reaction is conducted in THF at 80−90 °C, imidoiron cubanes are obtained in quantity, but in three forms: the $Fe^{2+}Fe^{3+}{}_3$ cluster **49** as the dominant product, and the all-ferric cubane **50** and site-differentiated cubane **51** as minority components. The preferential formation of the reduced cluster **49** rather than the anticipated all-ferric **50** implicates the intervention of a redox buffer that ties the reduction of ferric centers to the oxidation of nitrogen anions or their coordinated equivalents. The remaining cubane product **51** is notable in possessing terminal imide coordination at one iron site; this moiety, unknown in iron chemistry prior to the synthesis of **51**, is distinguished structurally by a near linear Fe═N—R bond angle (178.6(3)°) with a short Fe═NR contact (1.635(4) Å) indicative of a multiple bond. By formal charge count, this cluster possesses an $[Fe_4(NR)_4]^{5+}$ core. Mössbauer spectroscopy revealed localized Fe^{III} and Fe^{IV} sites in a 3:1 ratio at 150 K.[145]

A very different product mixture occurs when the same reaction is conducted in diethyl ether without heating (Scheme 10).[146] Imidoiron clusters do not form to any significant extent; instead, two major species appear: mononuclear **52**, a ferrous complex that again demonstrates the existence of a facile redox process, and dinuclear diferric **53**. Dissolution of this mixture in DME, follow by expeditious (hours) crystallization at −30 °C, allows isolation of a metastable, mixed amide-/imide-ligated voided-cubane cluster **54**. Standing in solution over longer intervals leads exclusively to the reduced cubane **49** as the sole NMR-active product. Cluster **54** appears to be related to the starting components of the mixture by fragment condensation reaction 22. This relationship, in conjunction with the eventual conversion of the mononuclear/dinuclear mixture to the reduced cubane cluster in DME, suggests a cluster assembly pathway, proceeding from di- to tri- to the final tetranuclear cubane geometry (eqs 22 and 23); ether solvent appears to halt the cluster assembly at an early stage. In an independent investigation, Fenske and co-workers[147] have also obtained dinuclear and cubane-type imidoiron clusters through similar reactions.

$$[Fe_2(\mu_2\text{-}NBu^t)_2Cl_4]^{2-} + [FeCl_2(NH_2Bu^t)_2] \rightarrow [Fe_3(\mu_3\text{-}NBu^t)(\mu_2\text{-}NBu^t)(\mu_2\text{-}NHBu^t)_2Cl_3]^- + 2H^+ + 3Cl^- \quad (22)$$

$$[Fe_2(\mu_2\text{-}NBu^t)_2Cl_4]^{2-} + [Fe_3(\mu_3\text{-}NBu^t)(\mu_2\text{-}NBu^t)\text{-}(\mu_2\text{-}NHBu^t)_2Cl_3]^- + 2H^+ + Cl^- \rightarrow [Fe_4(\mu_3\text{-}NBu^t)_4Cl_4]^- + [FeCl_4]^- + 2Bu^tNH_2 \quad (23)$$

The marked basicity of nitrogen anions such as the alkylamide used in Scheme 10 makes them aggressive reagents that are easily protonated or oxidized, and incompatible with the polar solvents typically used for the synthesis of charged clusters. To counter these perceived limitations and provide an alternative synthetic entry, the silylamide protonolysis methodology employed in Scheme 9 was applied via the heteroleptic ferric precursor **55** in Scheme 11.[148] Protonolysis with 1 equiv of aniline in THF results in the isolation of the complex cluster salt **56**, which consists of two diferrous monocations and a tri-

Scheme 11. Synthetic Routes to the Imidochloro Species Dinuclear 57 and Linear Trinuclear 58 Containing Two Fe^{III} and One Fe^{IV}

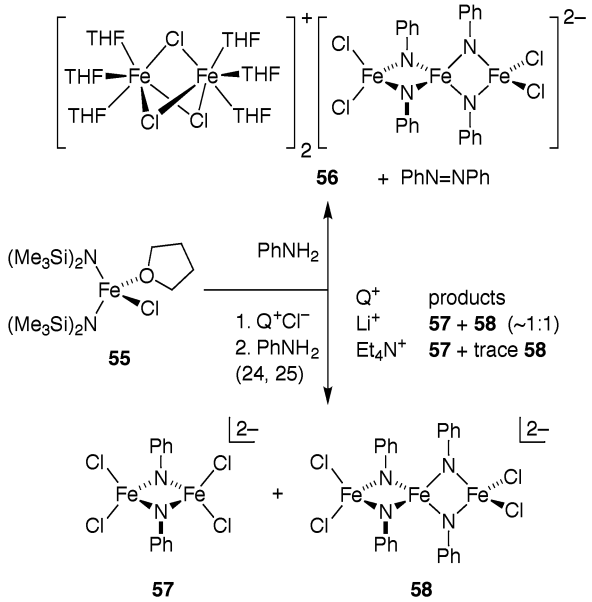

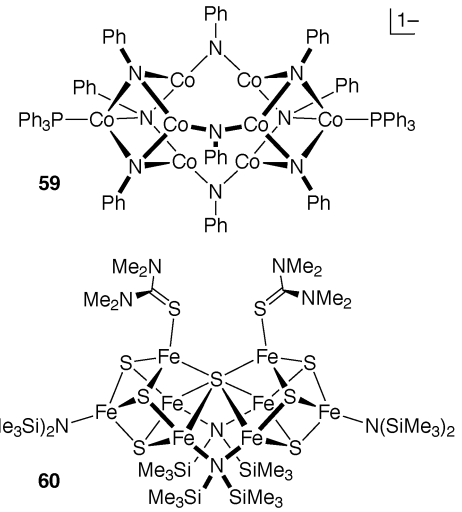

Figure 7. Nitrogen-anion-ligated structural relatives of the nitrogenase clusters, $[Co_8(NPh)_9(PPh_3)_2]^-$ (**59**) and $[Fe_8S_7(N(SiMe_3)_2)_4(S{=}C(NMe_2)_2)_2]$ (**60**). The $[Co_8(\mu_3\text{-}NPh)_6(\mu_2\text{-}NPh)_3]^-$ core of **59** is homologous to the $[MoFe_7(\mu_3\text{-}S)_6(\mu_2\text{-}S)_3]^z$ framework of the FeMo-co core, less the interstitial atom; amide-ligated cluster **60** and the P^N cluster share the same $[Fe_8(\mu_3\text{-}S)_6(\mu_6\text{-}S)]^z$ core motif.

nuclear imidoiron dianion, along with quantities of azobenzene that make explicit the redox connection, previously surmised, between nitrogen and iron. This redox chemistry, however, can be controlled through the use of appropriate co-reagents. The introduction of 1 equiv of lithium chloride prior to protonolysis by aniline diminishes subsequent azobenzene formation to trace levels and produces two dianionic clusters, dinuclear **57** and trinuclear **58**, as lithium salts in roughly equimolar amounts. Hypothetical balanced reactions can be formulated for the generation of both clusters using the exact experimental stoichiometry (eqs 24 and 25); eq 25 is noteworthy in coupling the

$$2[FeCl(N(SiMe_3)_2)_2(THF)] + 2Cl^- + 2ArNH_2 \rightarrow [Fe_2(\mu_2\text{-}NAr)_2Cl_4]^{2-} + 4HN(SiMe_3)_2 + 2THF \quad (24)$$

$$4[FeCl(N(SiMe_3)_2)_2(THF)] + 4Cl^- + 4ArNH_2 \rightarrow [Fe_3(\mu_3\text{-}NAr)_4Cl_4]^{2-} + [FeCl_4]^{2-} + 4THF \quad (25)$$

reduction of Fe^{III} to Fe^{II} (which goes undetected in the synthesis) to the formation of an oxidized cluster formally consisting of two Fe^{III} and one Fe^{IV}. The isolation of **58** and its spectroscopic identity with the imidoiron cluster of **56** prove the earlier charge formulation for the components in **56**. The role of lithium chloride is varied: the chloride coordinates to iron, thereby moderating ligand substitution chemistry and inhibiting runaway oligomerization; the anionic complexes generated by chloride coordination are less prone to reduction to the ferrous state; and the lithium provides a counterion to solubilize these anionic complexes. Cluster assembly can be further controlled if Et_4NCl is used in place of LiCl; protonolysis under these conditions gives almost exclusively the Et_4N^+ version of dinuclear **57**. This behavior suggests a stepwise path for cluster formation, from mono- to di- to trinuclear species, where chloride loss, which can be assisted by direct interaction with the hard Li^+ cation, must precede nuclearity expansion.

4.2.2. Imidoiron Chemistry: Generalizations

The chemistry of weak-field imidoiron complexes parallels in many respects the well-established chemistry of iron−sulfur systems.[1,148] The similarity is most obvious in the cluster structures, where the linear di- and trinuclear clusters and the tetranuclear cubanes all have corresponding sulfidoiron counterparts. The amidoimido voided cubane **54** is equivalent to a diprotonated Fe_3S_4 voided cubane core; sulfide protonation, in fact, is believed to occur in certain biological clusters of that geometry.[149] The structural equivalence of imide and sulfide extends to the curious imidocobalt cluster **59** in Figure 7, prepared by the reaction of $CoCl_2$ with Ph_3P and Li_2-NPh in a 2:1:2.67 ratio, that bears a remarkable resemblance to the pre-interstitial version of FeMo-co.[150] The analogy also applies to chemical reactivity: the iron-mediated redox transformations of nitrogen species echo the sulfur/sulfide and disulfide/thiolate interconversions that are prevalent throughout the synthetic chemistry of iron−sulfur clusters.[1,151]

There is no a priori basis to expect congruent chemistries for imide and sulfide. The two ligands share the same charge, but they are neither isoelectronic nor isosteric, and physicochemical properties such as basicity and donor ability differ considerably. Indeed, the latter contrast is quite evident in the stabilization of the uncommon Fe^{IV} oxidation state in clusters **51**, **56**, and **58**, and in the general tendency toward more oxidized cores for imidoiron species when comparing structurally equivalent imide and sulfide clusters. The a posteriori connection between the two ligand systems nonetheless provides a useful conceptual framework to guide further synthetic endeavors, particularly as they might be translated and applied to nitride chemistry.

4.2.3. Clusters with Mixed Nitrogen Anion/Sulfide Ligands

The integration of nitrogen anion and sulfide cluster chemistries is a logical next step in the evolution of FeMo-co-directed synthesis. Such studies can approximate, to varying degrees, the weak-field nitridosulfidoiron environment of the biological cluster; in so doing, they delineate the essential properties of relevant hybrid coordination spheres, while advancing methods and precursors for the construction of higher fidelity analogues. Research in this area is current and ongoing, as demonstrated by the examples that follow.

The Fe_4S_4 cubane-type core is the most extensively investigated, indeed, archetypal, cluster motif in iron−sulfur chemistry.[1,151] It therefore serves as an ideal reference platform to evaluate the influence of nitrogen anion ligands on an iron−sulfur cluster.[152] The stoichiometric self-assembly reaction 26 of mononuclear **55** and NaSH allows facile access to an all-ferric cubane capped by terminal amide ligation. Reduction with 0.25 and 1 equiv of Na_2S yields the

$$4[FeCl(N(SiMe_3)_2)_2(THF)] + 4NaSH \rightarrow [Fe_4S_4(N(SiMe_3)_2)_4] + 4NaCl + 4HN(SiMe_3)_2 \quad (26)$$

one- and two-electron reduced clusters, $[Fe_4S_4(N(SiMe_3)_2)_4]^-$ and $[Fe_4S_4(N(SiMe_3)_2)_4]^{2-}$, respectively. In general, the properties of these amide-ligated clusters are similar to those of other weak-field Fe_4S_4 complexes except in relation to redox potentials and oxidation states. The clusters form the redox series 27, with $E_{1/2}(0/1-) = 0.38$ V and $E_{1/2}(1-/2-) = -0.50$ V vs SCE in 9:1 v/v acetonitrile/benzene. In contrast,

$$[Fe_4S_4(N(SiMe_3)_2)_4]^{2-} \leftrightarrow [Fe_4S_4(N(SiMe_3)_2)_4]^{-} \leftrightarrow [Fe_4S_4(N(SiMe_3)_2)_4] \quad (27)$$

the $z = 1-$ member of the generalized redox series $[Fe_4S_4(SR)_4]^z$ is sometimes detectable electrochemically but, with one exception,[153] is too unstable to isolate. Further, the $z = 0$ cluster is unknown. The isolation of the all-ferric $[Fe_4S_4]^{4+}$ core is limited strictly to $[Fe_4S_4(N(SiMe_3)_2)_4]$ and to the strong-field, cyclopentadienyl-ligated cubanes.[154] The stability of $[Fe_4S_4]^{3+,4+}$ clusters depends on three factors: intrinsic donor ability of the terminal ligands, resistance of these ligands to oxidation (with accompanying core reduction), and steric protection of the core from attack by solvent or another nucleophile. Evidently, bis(trimethylsilyl)amide fulfills these requirements.

Amide ligation also appears in the high-nuclearity iron−sulfur cluster **60**[155] (Figure 7), of immediate relevance not to FeMo-co but to the P cluster. This complex, prepared by the complicated assembly system 8[Fe((N(SiMe$_3$)$_2$)$_2$]/3(Me$_2$N)$_2$CS/12 2,4,6-Pr$^i_3$C$_6$H$_2$-SH/7S, contains the same iron−sulfur core geometry and ligand positioning observed in the P^N state of the P cluster, albeit with different external ligands. The synthetic cluster shows a core oxidation level that corresponds to the two-electron oxidized P^{OX}, rather than the P^N, state; in the macromolecular structures, the P^{OX} cluster shows a different, rearranged geometry relative to the P^N cluster.[20,21] Cluster **60** is reported to be unstable in solution. The roles of the various components in cluster formation are unclear at this time. The isolation of **60**, however, does demonstrate again the fundamental accessibility and stability of the P^N core structure.

Scheme 12. Synthesis of Clusters with Mixed Nitrogen Anion/Sulfide Ligands: Dinuclear 62 and Cubane-type 63

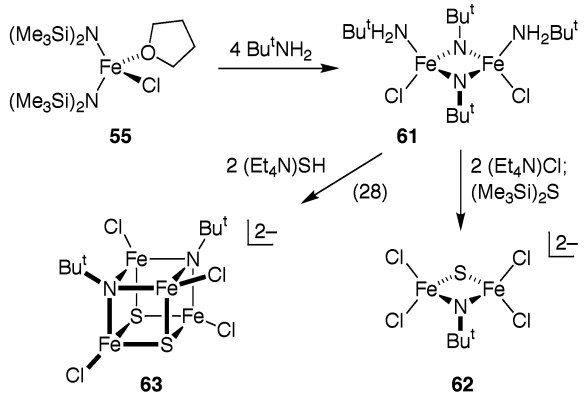

The discovery of the interstitial, non-sulfide ligand in FeMo-co necessitates the development of methods for the construction of mixed-ligand cores. Initial progress toward this end has been accomplished by extension of imidoiron cluster chemistry, as depicted in Scheme 12.[156] The reaction of mononuclear **55** with excess Bu^tNH_2 allows isolation of the neutral diferric amine−imide complex **61**. Treatment of this dimer with 2:1 $Et_4NCl/(Me_3Si)_2S$ yields the dinuclear imidosulfido complex **62**. As expected from the weak-field iron environment, the replacement of core imide by sulfide is not completely selective for the monosubstituted complex, and disubstituted $[Fe_2S_2Cl_4]^{2-}$ is detectable as a reaction product; the crystallinity of **62**, however, allows its isolation in good yield. Higher nuclearity clusters with mixed imide/sulfide cores are also attainable: the reaction of **61** with 2 equiv of $(Et_4N)(SH)$ leads to the formation of the dianionic cubane **63**. The balanced reaction 28 can be offered, in which iron reduction is coupled to azobutane formation.

$$2[Fe_2(\mu_2\text{-}NBu^t)_2Cl_2(NH_2Bu^t)_2] + 2HS^- \rightarrow [Fe_4(\mu_3\text{-}NBu^t)_2(\mu_3\text{-}S)_2Cl_4]^{2-} + 5Bu^tNH_2 + {}^1/_2Bu^tN{=}NBu^t \quad (28)$$

5. Synthetic Methodology: An Overview

Despite the progress delineated in this review, the synthetic challenge posed by the nitrogenase metalloclusters with their intrinsic property constraints remains formidable. The target molecules consist largely or exclusively of weak-field $Fe^{II,III}$ sites. As a consequence, coordination environments are labile, sites are locally paramagnetic but magnetically coupled, metal centers and sulfur ligands are redox-active, and clusters typically have marked sensitivity or, at best, limited stability upon exposure to dioxygen or water. Because of instability, column chromatography of both neutral molecules and cluster salts is not useful, and final purity is generally achieved by careful anaerobic extraction and recrystallization

protocols. Cluster paramagnetism can produce characteristic spectroscopic signatures, but these require for interpretation full structure disclosure by crystallographic means.

Notwithstanding these obstacles, the 25 years of synthesis and reactivity have advanced many fundamental aspects of the problem. The largely empirical enterprise of cluster synthesis can be brought under the governance of rational chemical manipulation and tactics. Three general, conceptual strategies for cluster synthesis have evolved and are summarized below with examples.

(i) *Self-assembly*, the self-organizing synthesis of clusters from simple mononuclear precursors and ligand reagents, provides the cornerstone approach for cluster synthesis. Although the reaction outcome is empirical, an understanding of the underlying chemistry and the cognizant choice of parameters—i.e., precursors, stoichiometry, reaction conditions—are essential to a favorable outcome. The selective, highly optimized syntheses of MFe_3S_4 (**1**−**4**, Scheme 1) and MFe_4S_6 (**23**, Scheme 4) clusters are outstanding examples of the efficacy of self-assembly, as is the formation of iron−sulfur clusters from simple reactants.[1,151] The recent synthesis of the P-cluster analogue **60**[153] is yet another demonstration of the attainment of a complicated but thermodynamically stable structure by self-assembly.

(ii) *Fragment condensation* involves the coupling of pre-existing di- or polynuclear clusters or a cluster with a mononuclear reactant to give higher-nuclearity clusters of (in theory) predictable geometries. As such, it is a more systematic cluster synthesis strategy than self-assembly since the structural relationship between starting materials and products is meant to be explicit. Reactions classified as fragment condensations range from face capping (synthesis of **13**, Figure 4) to intercluster bridging (formation of double cubanes **28**−**30**, Scheme 5) to more substantial core fusion (synthesis of edge-bridged double cubanes **31**, **38**, and **43**, Schemes 6−8). Fragment condensation has served as the primary method to synthesize clusters with appropriate core nuclearities.

(iii) *Core rearrangement* is the reorganization of a pre-existing cluster to a different core geometry. Such structural changes can be induced through redox reactions or by changes in ligand set through reaction with an external reagent. The existence of core rearrangement reactions cannot be securely predicted in advance; instead, the utility of the method rests on the assumption that stable target geometries and their compositional or near-compositional isomers (i.e., the precursor cluster) are related by accessible intramolecular reaction pathways. The hydrosulfide-induced transformations of octanuclear edge-bridged double cubanes to the P-cluster topology (**32** and **33**, Scheme 6; **40** and **44**, Schemes 7 and 8) are convincing demonstrations of this behavior.

A fourth approach to cluster synthesis, *cluster excision*, relies on the existence of solid-state materials containing discrete cluster motifs as repeat units within an extended polymeric lattice; removal of these clusters from the solid—excision—allows their molecular access.[157] This approach appears to be inapplicable to iron−sulfur species because clustering is unknown for iron−sulfide phases.

The foregoing strategies are not mutually exclusive when put to practice. For example, the self-assembly of VFe_3S_4 cluster **17** (Scheme 3) in effect results from fragment condensation of $FeCl_2$ with **16**, followed by core rearrangement to the cubane geometry. The foregoing cluster synthesis strategies are not mechanistic statements, and, indeed, it would be unwise to assume so, given the difficulty in obtaining reliable mechanistic data on weak-field cluster assembly. Instead, they serve primarily as elements of a conceptual framework to guide the planning of synthesis and the organization of synthetic methods. This matter is well demonstrated by the orderly development of synthetic routes to imidoiron clusters, a heretofore unexplored molecular class of already impressive diversity.

Much of the foregoing research has been intended to contribute to the chemical understanding of biometallocenters by deriving methods for the synthesis of their analogues. The intent of this work differs not at all from the total synthesis of organic natural products which in one view "combines target-oriented synthesis with the discovery and development of new synthetic technologies".[158] The often empirical nature of cluster synthesis should not be a deterrent to experimentation for, as Pasteur observed, "serendipity...appears to be most generous to those positioned to detect and exploit the accidental". In this context, it should be borne in mind that the biosynthetic pathway of not one polynuclear metal center in biology has yet been elucidated. The biosynthesis of metallocenters is now a forefront area of inquiry.[159,160] It remains to be seen whether the synthesis of nitrogenase clusters, faithful in their entirety to the native clusters, will precede or follow explication of the biosynthetic pathways. The results presented here allow optimism that the former will be the case.

6. Acknowledgments

Research on biologically related metal clusters has been supported in the authors' laboratories by grants NSF CHE-9984645 (to S.C.L.) and NIH GM 28856 (to R.H.H.) This article is dedicated to the memory of Barbara K. Burgess.

7. Abbreviations

bpy	2,2′-bipyridine
cat	catecholate(2−) or substituted catecholate(2−)
cit	citrate
Cl_4cat	tetrachlorocatecholate(2−)
co	cofactor
CODH	carbon monoxide dehydrogenase
DMA	*N*,*N*′-dimethylacetamide
DME	1,2-dimethoxyethane
dmpe	1,2-bis(dimethylphosphino)ethane
LS_3	1,3,5-tris((4,6-dimethyl-3-mercaptophenyl)thio-2,4,6- tris(*p*-tolylthio)benzene(3−)
Meida	*N*-methylimidodiacetate(2−)
NMF	*N*-methylformamide
py	pyridine
SCE	standard calomel electrode

Tp	tris(pyrazolyl)hydroborate(1−)
XAS	X-ray absorption spectroscopy

8. References

(1) Venkateswara Rao, P.; Holm, R. H. *Chem. Rev.* **2004**, *104*, 527 (in this issue).
(2) Holm, R. H. *Pure Appl. Chem.* **1995**, *67*, 217.
(3) Howard, J. B.; Rees, D. C. *Chem. Rev.* **1996**, *96*, 2965.
(4) Burgess, B. K.; Lowe, D. J. *Chem. Rev.* **1996**, *96*, 2983.
(5) Eady, R. R. *Chem. Rev.* **1996**, *96*, 3013.
(6) Smith, B. E. *Adv. Inorg. Chem.* **1999**, *47*, 160.
(7) Christiansen, J.; Dean, D. R.; Seefeldt, L. C. *Annu. Rev. Plant Physiol. Plant Mol. Biol.* **2001**, *52*, 269.
(8) Crane, B. R.; Siegel, L. M.; Getzoff, E. D. *Science* **1995**, *270*, 59.
(9) Crane, B. R.; Siegel, L. M.; Getzoff, E. D. *Biochemistry* **1997**, *36*, 12120.
(10) Peters, J. W.; Lanzilotta, W. N.; Lemon, B. J.; Seefeldt, L. C. *Science* **1998**, *282*, 1853.
(11) Nicolet, Y.; Lemon, B. J.; Fontecilla-Camps, J. C.; Peters, J. W. *Trends Biochem. Sci.* **2000**, *25*, 138.
(12) Volbeda, A.; Charon, M.-C.; Piras, C.; Hatchikian, E. C.; Frey, M.; Fontecilla-Camps, J. C. *Nature* **1995**, *373*, 580.
(13) Ogata, H.; Mizoguchi, Y.; Mizuno, N.; Miki, K.; Adachi, S.; Yasuoka, N.; Yagi, T.; Yamauchi, O.; Hirota, S.; Higuchi, Y. *J. Am. Chem. Soc.* **2002**, *124*, 11628.
(14) Matias, P. M.; Soares, C. M.; Saraiva, L. M.; Coelho, R.; Marais, J.; Le Gall, J.; Carrondo, M. A. *J. Biol. Inorg. Chem.* **2001**, *6*, 63.
(15) Dobbek, H.; Svetlitchnyi, V.; Gremer, L.; Huber, R.; Meyer, O. *Science* **2001**, *293*, 1281.
(16) Drennan, C. L.; Heo, J.; Sintchak, M. D.; Schreiter, E.; Ludden, P. W. *Proc. Natl. Acad. Sci. U.S.A.* **2001**, *98*, 11973.
(17) Doukov, T. I.; Iverson, T. M.; Seravalli, J.; Ragsdale, S. W.; Drennan, C. L. *Science* **2002**, *298*, 567.
(18) Darnault, C.; Volbeda, A.; Kim, E. J.; Legrand, P.; Vernede, X.; Lindahl, P. A.; Fontecilla-Camps, J. C. *Nature Struct. Biol.* **2003**, *10*, 271.
(19) Dobbek, H.; Gremer, L.; Kiefersauer, R.; Huber, R.; Meyer, O. *Proc. Natl. Acad. Sci. U.S.A.* **2002**, *99*, 15971.
(20) Peters, J. W.; Stowell, M. H. B.; Soltis, S. M.; Finnegan, M. G.; Johnson, M. K.; Rees, D. C. *Biochemistry* **1997**, *36*, 1181.
(21) Mayer, S. M.; Lawson, D. M.; Gormal, C. A.; Roe, S. M.; Smith, B. E. *J. Mol. Biol.* **1999**, *292*, 871.
(22) Einsle, O.; Tezcan, F. A.; Andrade, S.; Schmid, B.; Yoshida, M.; Howard, J. B.; Rees, D. C. *Science* **2002**, *297*, 1696.
(23) Kim, J.; Rees, D. C. *Nature* **1992**, *360*, 553.
(24) Chan, M. K.; Kim, J.; Rees, D. C. *Science* **1993**, *260*, 792.
(25) Müller, A.; Diemann, E.; Jostes, R.; Bögge, H. *Angew. Chem., Int. Ed. Engl.* **1981**, *20*, 934.
(26) Coucouvanis, D. *Acc. Chem. Res.* **1981**, *14*, 201.
(27) Holm, R. H.; Simhon, E. D. In *Molybdenum Enzymes*; Spiro, T. G., Ed.; Wiley: New York, 1985; pp 1−87.
(28) Eldredge, P. A.; Averill, B. A. *J. Cluster Sci.* **1990**, *1*, 269.
(29) Eldredge, P. A.; Bose, K. S.; Barber, D. E.; Bryan, R. F.; Sinn, E.; Rheingold, A.; Averill, B. A. *Inorg. Chem.* **1991**, *30*, 2365.
(30) Barber, D. E.; Bryan, R. F.; Sabat, M.; Bose, K. S.; Averill, B. A. *Inorg. Chem.* **1996**, *35*, 4635.
(31) Garner, C. D.; Acott, S. R.; Christou, G.; Collison, D.; Mabbs, F. E.; Petrouleas, V. *Philos. Trans. R. Soc. London A* **1982**, *308*, 159.
(32) Coucouvanis, D. *Acc. Chem. Res.* **1991**, *24*, 1.
(33) Malinak, S. M.; Coucouvanis, D. *Prog. Inorg. Chem.* **2001**, *49*, 592.
(34) Coucouvanis, D., private communication.
(35) Lee, S. C.; Holm, R. H. *Proc. Natl. Acad. Sci. U.S.A.* **2003**, *100*, 3595.
(36) Shah, V. K.; Brill, W. J. *Proc. Natl. Acad. Sci. U.S.A.* **1977**, *74*, 3249.
(37) Burgess, B. K. *Chem. Rev.* **1990**, *90*, 1377.
(38) Eady, R. R. *Coord. Chem. Rev.* **2003**, *237*, 23.
(39) Krahn, E.; Weiss, B. J. R.; Kröckel, M.; Groppe, J.; Henkel, G.; Cramer, S. P.; Trautwein, A. X.; Schneider, K.; Müller, A. *J. Biol. Inorg. Chem.* **2002**, *7*, 37.
(40) Lovell, T.; Torres, R. A.; Han, W.-G.; Liu, T.; Case, D. A.; Noodleman, L. *Inorg. Chem.* **2002**, *41*, 5744.
(41) Smith, B. E.; Eady, R. R.; Lowe, D. J.; Gormal, C. *Biochem. J.* **1988**, *250*, 299.
(42) Cramer, S. P.; Gillum, W. O.; Hodgson, K. O.; Mortenson, L. E.; Stiefel, E. I.; Chisnell, J. R.; Brill, W. J.; Shah, V. K. *J. Am. Chem. Soc.* **1978**, *100*, 3814.
(43) Cramer, S. P.; Hodgson, K. O.; Gillum, W. O.; Mortenson, L. E. *J. Am. Chem. Soc.* **1978**, *100*, 3398.
(44) Antonio, M. R.; Teo, B.-K.; Orme-Johnson, W. H.; Nelson, M. J.; Groh, S. E.; Lindahl, P. A.; Kauzlarich, S. M.; Averill, B. A. *J. Am. Chem. Soc.* **1982**, *104*, 4703.
(45) Eidsness, M. K.; Flank, A. M.; Smith, B. E.; Flood, A. C.; Garner, C. D.; Cramer, S. P. *J. Am. Chem. Soc.* **1986**, *108*, 2746.
(46) McLean, P. A.; True, A. E.; Nelson, M. J.; Chapman, S.; Godfrey, M. R.; Teo, B. K.; Orme-Johnson, W. H.; Hoffman, B. M. *J. Am. Chem. Soc.* **1987**, *109*, 943.
(47) Conradson, S. D.; Burgess, B. K.; Newton, W. E.; Mortenson, L. E.; Hodgson, K. O. *J. Am. Chem. Soc.* **1987**, *109*, 7507.
(48) Arber, J. M.; Flood, A. C.; Garner, C. D.; Gormal, C. A.; Hasnain, S. S.; Smith, B. E. *Biochem. J.* **1988**, *252*, 421.
(49) Holm, R. H. *Acc. Chem. Res.* **1977**, *10*, 427.
(50) Holm, R. H.; Ibers, J. A. In *Iron−Sulfur Proteins*; Lovenberg, W., Ed.; Academic Press: New York, 1997; Chapter 7.
(51) Herskovitz, T.; Averill, B. A.; Holm, R. H.; Ibers, J. A.; Phillips, W. D.; Weiher, J. F. *Proc. Natl. Acad. Sci. U.S.A.* **1972**, *69*, 2437.
(52) Averill, B. A.; Herskovitz, T.; Holm, R. H.; Ibers, J. A. *J. Am. Chem. Soc.* **1973**, *95*, 3523.
(53) Christou, G.; Garner, C. D. *J. Chem. Soc., Dalton Trans.* **1979**, 1093.
(54) Wolff, T. E.; Berg, J. M.; Warrick, C.; Hodgson, K. O.; Holm, R. H.; Frankel, R. B. *J. Am. Chem. Soc.* **1978**, *100*, 4630.
(55) Wolff, T. E.; Berg, J. M.; Hodgson, K. O.; Frankel, R. B.; Holm, R. H. *J. Am. Chem. Soc.* **1979**, *101*, 4140.
(56) Wolff, T. E.; Berg, J. M.; Power, P. P.; Hodgson, K. O.; Holm, R. H. *Inorg. Chem.* **1980**, *19*, 430.
(57) Wolff, T. E.; Power, P. P.; Frankel, R. B.; Holm, R. H. *J. Am. Chem. Soc.* **1980**, *102*, 4694.
(58) Christou, G.; Garner, C. D. *J. Chem. Soc., Dalton Trans.* **1980**, 2354.
(59) Christou, G.; Mascharak, P. K.; Armstrong, W. H.; Papaefthymiou, G. C.; Frankel, R. B.; Holm, R. H. *J. Am. Chem. Soc.* **1982**, *104*, 2820.
(60) Hagen, K. S.; Reynolds, J. G.; Holm, R. H. *J. Am. Chem. Soc.* **1981**, *103*, 4054.
(61) Greaney, M. A.; Coyle, C. L.; Pilato, R. S.; Stiefel, E. I. *Inorg. Chim. Acta* **1991**, *189*, 81.
(62) Christou, G.; Collison, D.; Garner, C. D.; Acott, S. R.; Mabbs, F. E.; Petrouleas, V. *J. Chem. Soc., Dalton Trans.* **1982**, 1575.
(63) Palermo, R. E.; Power, P. P.; Holm, R. H. *Inorg. Chem.* **1982**, *21*, 173.
(64) Henderson, R. A.; Oglieve, K. E. *J. Chem. Soc., Dalton Trans.* **1993**, 1467.
(65) Barrière, F.; Evans, D. J.; Hughes, D. L.; Ibrahim, S. K.; Talarmin, J.; Pickett, C. J. *J. Chem. Soc., Dalton Trans.* **1999**, 957.
(66) Chen, C.; Wen, T.; Li, W.; Zhu, H.; Chen, Y.; Liu, Q.; Lu, J. *Inorg. Chem.* **1999**, *38*, 2375.
(67) Christou, G.; Garner, C. D.; Miller, R. M.; Johnson, C. E.; Rush, J. D. *J. Chem. Soc., Dalton Trans.* **1980**, 2363.
(68) Rutstrom, D. J.; Robbat, A., Jr. *J. Electroanal. Chem. Interfacial Electrochem.* **1986**, *200*, 193.
(69) Yamamura, T.; Christou, G.; Holm, R. H. *Inorg. Chem.* **1983**, *22*, 939.
(70) Holm, R. H. *Chem. Soc. Rev.* **1981**, *10*, 455.
(71) Armstrong, W. H.; Holm, R. H. *J. Am. Chem. Soc.* **1981**, *103*, 6246.
(72) Armstrong, W. H.; Mascharak, P. K.; Holm, R. H. *J. Am. Chem. Soc.* **1982**, *104*, 4373.
(73) Mascharak, P. K.; Armstrong, W. H.; Mizobe, Y. *J. Am. Chem. Soc.* **1983**, *105*, 475.
(74) Palermo, R. E.; Singh, R.; Bashkin, J. K.; Holm, R. H. *J. Am. Chem. Soc.* **1984**, *106*, 2600.
(75) Huang, J.; Goh, C.; Holm, R. H. *Inorg. Chem.* **1997**, *36*, 356.
(76) Armstrong, W. H.; Mascharak, P. K.; Holm, R. H. *Inorg. Chem.* **1982**, *21*, 1699.
(77) Zhang, Y.-P.; Bashkin, J. K.; Holm, R. H. *Inorg. Chem.* **1987**, *36*, 694.
(78) Liu, Q.-T.; Huang, L.-R.; Kang, B.-S.; Liu, C.-W.; Wang, L.-L.; Lu, J.-X. *Acta Chim. Sin.* **1986**, *44*, 107.
(79) Liu, Q.; Huang, L.; Liu, H.; Lei, X.; Wu, D.; Kang, B.; Lu, J. *Inorg. Chem.* **1990**, *29*, 4131.
(80) Mascharak, P. K.; Papaefthymiou, G. C.; Armstrong, W. H.; Foner, S.; Frankel, R. B.; Holm, R. H. *Inorg. Chem.* **1983**, *22*, 2851.
(81) Carney, M. J.; Kovacs, J. A.; Zhang, Y.-P.; Papaefthymiou, G. C.; Spartalian, K.; Frankel, R. B.; Holm, R. H. *Inorg. Chem.* **1987**, *26*, 719.
(82) Palermo, R. E.; Holm, R. H. *J. Am. Chem. Soc.* **1983**, *105*, 4310.
(83) Mizobe, Y.; Mascharak, P. K.; Palermo, R. E.; Holm, R. H. *Inorg. Chim. Acta* **1983**, *80*, L65.
(84) Demadis, K. D.; Coucouvanis, D. *Inorg. Chem.* **1995**, *34*, 436.
(85) Coucouvanis, D.; Kanatzidis, M. G. *J. Am. Chem. Soc.* **1985**, *107*, 5005.
(86) Coucouvanis, D.; Salifoglou, A.; Kanatzidis, M. G.; Dunham, W. R.; Simopoulos, A.; Kostikas, A. *Inorg. Chem.* **1988**, *27*, 4066.
(87) Al-Ahmad, S.; Salifoglou, A.; Kanatzidis, M. G.; Dunham, W. R.; Coucouvanis, D. *Inorg. Chem.* **1990**, *29*, 927.
(88) Kovacs, J. A.; Bashkin, J. K.; Holm, R. H. *J. Am. Chem. Soc.* **1985**, *107*, 1784.
(89) Demadis, K. D.; Coucouvanis, D. *Inorg. Chem.* **1994**, *19*, 4195.

(90) Mosier, P. E.; Kim, C. G.; Coucouvanis, D. *Inorg. Chem.* **1993**, *32*, 2620.
(91) Kovacs, J. A.; Holm, R. H. *J. Am. Chem. Soc.* **1986**, *108*, 340.
(92) Kovacs, J. A.; Holm, R. H. *Inorg. Chem.* **1987**, *26*, 702.
(93) Kovacs, J. A.; Holm, R. H. *Inorg. Chem.* **1987**, *26*, 711.
(94) Zhu, H.-P.; Liu, Q.-T.; Chen, C.-N. *Chin. J. Struct. Chem.* **2001**, *20*, 19.
(95) Deng, Y.; Liu, Q.; Chen, C.; Wang, Y.; Cai, Y.; Wu, D.; Kang, B.; Liao, D.; Cui, J. *Polyhedron* **1997**, *16*, 4121.
(96) Coucouvanis, D.; Al-Ahmad, S.; Salifoglou, A.; Dunham, W. R.; Sands, R. H. *Angew. Chem., Int. Ed.* **1988**, *27*, 1353.
(97) Coucouvanis, D.; Al-Ahmad, S. A.; Salifoglou, A.; Papaefthymiou, V.; Kostikas, A.; Simopoulos, A. *J. Am. Chem. Soc.* **1992**, *114*, 2472.
(98) Raebiger, J. W.; Crawford, C. A.; Zhou, J.; Holm, R. H. *Inorg. Chem.* **1997**, *36*, 994.
(99) Ciurli, S.; Ross, P. K.; Scott, M. J.; Yu, S.-B.; Holm, R. H. *J. Am. Chem. Soc.* **1992**, *114*, 5415.
(100) Zhou, J.; Scott, M. J.; Hu, Z.; Peng, G.; Münck, E.; Holm, R. H. *J. Am. Chem. Soc.* **1992**, *114*, 10843.
(101) Malinak, S. M.; Demadis, K. D.; Coucouvanis, D. *J. Am. Chem. Soc.* **1995**, *117*, 3126.
(102) Huang, J.; Mukerjee, S.; Segal, B. M.; Akashi, H.; Zhou, J.; Holm, R. H. *J. Am. Chem. Soc.* **1997**, *119*, 8662.
(103) Ciurli, S.; Holm, R. H. *Inorg. Chem.* **1989**, *28*, 1685.
(104) Snyder, B. S.; Holm, R. H. *Inorg. Chem.* **1988**, *27*, 2339.
(105) Reynolds, M. S.; Holm, R. H. *Inorg. Chem.* **1988**, *27*, 4494.
(106) Snyder, B. S.; Holm, R. H. *Inorg. Chem.* **1990**, *29*, 274.
(107) Noda, I.; Snyder, B. S.; Holm, R. H. *Inorg. Chem.* **1986**, *25*, 3851.
(108) Nordlander, E.; Lee, S. C.; Cen, W.; Wu, Z. Y.; Natoli, C. R.; Di Cicco, A.; Filipponi, A.; Hedman, B.; Hodgson, K. O.; Holm, R. H. *J. Am. Chem. Soc.* **1993**, *115*, 5549.
(109) Cen, W.; MacDonnell, F. M.; Scott, M. J.; Holm, R. H. *Inorg. Chem.* **1994**, *33*, 5809.
(110) Chu, C. T. W.; Dahl, L. F. *Inorg. Chem.* **1977**, *16*, 3245.
(111) Scott, M. J.; Holm, R. H. *Angew. Chem., Int. Ed. Engl.* **1993**, *32*, 564.
(112) Goh, C.; Holm, R. H. *Inorg. Chim. Acta* **1998**, *270*, 46.
(113) Tyson, M. A.; Coucouvanis, D. *Inorg. Chem.* **1997**, *36*, 3808.
(114) Han, J.; Beck, K.; Ockwig, N.; Coucouvanis, D. *J. Am. Chem. Soc.* **1999**, *121*, 10448.
(115) Coucouvanis, D.; Han, J.; Moon, N. *J. Am. Chem. Soc.* **2002**, *124*, 216.
(116) Stack, T. D. P.; Carney, M. J.; Holm, R. H. *J. Am. Chem. Soc.* **1989**, *111*, 1670.
(117) Challen, P. R.; Koo, S. M.; Dunham, W. R.; Coucouvanis, D. *J. Am. Chem. Soc.* **1990**, *112*, 2455.
(118) Huang, J.; Holm, R. H. *Inorg. Chem.* **1998**, *37*, 2247.
(119) Demadis, K. D.; Campana, C. F.; Coucouvanis, D. *J. Am. Chem. Soc.* **1995**, *117*, 7832.
(120) Osterloh, F.; Segal, B. M.; Achim, C.; Holm, R. H. *Inorg. Chem.* **2000**, *39*, 980.
(121) Goh, C.; Segal, B. M.; Huang, J.; Long, J. R.; Holm, R. H. *J. Am. Chem. Soc.* **1996**, *118*, 11844.
(122) Zhou, H.-C.; Holm, R. H. *Inorg. Chem.* **2003**, *42*, 11.
(123) Hauser, C.; Bill, E.; Holm, R. H. *Inorg. Chem.* **2002**, *41*, 1615.
(124) Han, J.; Koutmos, M.; Al-Ahmad, S.; Coucouvanis, D. *Inorg. Chem.* **2001**, *40*, 5985.
(125) Osterloh, F.; Achim, C.; Holm, R. H. *Inorg. Chem.* **2001**, *40*, 224.
(126) Schmid, B.; Ribbe, M. W.; Einsle, O.; Yoshida, M.; Thomas, L. M.; Dean, D. R.; Rees, D. C.; Burgess, B. K. *Science* **2002**, *296*, 352.
(127) Osterloh, F.; Sanakis, Y.; Staples, R. J.; Münck, E.; Holm, R. H. *Angew. Chem., Int. Ed.* **1999**, *38*, 2066.
(128) Zhang, Y.; Zuo, J.-L.; Zhou, H.-C.; Holm, R. H. *J. Am. Chem. Soc.* **2002**, *124*, 14292.
(129) Zhang, Y.; Holm, R. H. *J. Am. Chem. Soc.* **2003**, *125*, 3910.
(130) Seino, H.; Arai, Y.; Iwata, N.; Nagao, S.; Mizobe, Y.; Hidai, M. *Inorg. Chem.* **2001**, *40*, 1677.
(131) Fomitchev, D. V.; McLauchlan, C. C.; Holm, R. H. *Inorg. Chem.* **2002**, *41*, 958.
(132) Zuo, J.-L.; Zhou, H.-C.; Holm, R. H. *Inorg. Chem.* **2003**, *42*, 4624.
(133) Dance, I. *J. Chem. Soc., Chem. Commun.* **2003**, 324.
(134) Hinnemann, B.; Nørskov, J. K. *J. Am. Chem. Soc.* **2003**, *125*, 1466.
(135) Lovell, T.; Liu, T.; Case, D. A.; Noodleman, L. *J. Am. Chem. Soc.* **2003**, *125*, 8377.
(136) As is true for synthetic efforts, the utility of computational models requires both convincing calibration with and accurate input from experiment. These demands, however, are more stringent in silico inasmuch as the calculation of purely theoretical species is readily achieved.
(137) Lee, H.-I.; Benton, P. M. C.; Laryukhin, M.; Igarashi, R. Y.; Dean, D. R.; Seefeldt, L. C.; Hoffman, B. M. *J. Am. Chem. Soc.* **2003**, *125*, 5604.
(138) Gómaz-Sal, P.; Martin, A.; Mena, M.; Yélamos, C. *J. Chem. Soc., Chem. Commun.* **1995**, 2185.
(139) Zeller, E.; Beruda, H.; Kolb, A.; Bissinger, P.; Riede, J.; Schmidbaur, H. *Nature* **1991**, *352*, 141.
(140) Nugent, W. A.; Mayer, J. M. *Metal−Ligand Multiple Bonds*; Wiley-Interscience: New York, 1988.
(141) Fjare, D. E.; Gladfelter, W. L. *Inorg. Chem.* **1981**, *20*, 3533.
(142) Blohm, M. L.; Fjare, D. E.; Gladfelter, W. L. *Inorg. Chem.* **1983**, *22*, 1004.
(143) Verma, A. K.; Lee, S. C. *J. Am. Chem. Soc.* **1999**, *121*, 10838.
(144) Zdilla, M.; Verma, A. K.; Lee, S. C., manuscript in preparation.
(145) Verma, A. K.; Nazif, T. N.; Achim, C.; Lee, S. C. *J. Am. Chem. Soc.* **2001**, *122*, 11013.
(146) Duncan, J. S.; Traub, M. C.; Lee, S. C., manuscript in preparation.
(147) Link, H.; Decker, A.; Fenske, D. *Z. Anorg. Allg.Chem.* **2000**, *626*, 1567.
(148) Duncan, J. S.; Nazif, T. N.; Verma, A. K.; Lee, S. C. *Inorg. Chem.* **2003**, *42*, 1211.
(149) Chen, K.; Hirst, J.; Camba, R.; Bonagura, C. A.; Stout, C. D.; Burgess, B. K.; Armstrong, F. A. *Nature* **2000**, *405*, 814.
(150) Link, H.; Fenske, D. *Z. Anorg. Allg.Chem.* **1999**, *625*, 1878.
(151) Holm, R. H. In *Bio-coordination Chemistry*; Que, L., Jr., Tolman, W. A., Eds.; Comprehensive Coordination Chemistry; Elsevier: Amsterdam, 2003.
(152) Sharp, C. R.; Duncan, J. S.; Lee, S. C., manuscript in preparation.
(153) O'Sullivan, T.; Millar, M. M. *J. Am. Chem. Soc.* **1985**, *107*, 4096.
(154) Ogino, H.; Inomata, S.; Tobita, H. *Chem. Rev.* **1998**, *98*, 2093.
(155) Ohki, Y.; Sunada, Y.; Honda, M.; Katsada, M.; Tatsumi, K. *J. Am. Chem. Soc.* **2003**, *125*, 4052.
(156) Duncan, J. S.; Lee, S. C., manuscript in preparation.
(157) Lee, S. C.; Holm, R. H. *Angew. Chem., Int. Ed. Engl.* **1990**, *29*, 840.
(158) Nicolaou, K. C.; Vourloumis, D.; Wissinger, N.; Baran, P. S. *Angew. Chem., Int. Ed.* **2000**, *39*, 44.
(159) Hausinger, R. P. *Adv. Inorg. Biochem.* **1996**, *11*, 1.
(160) Frazzon, J.; Dean, D. R. *Curr. Opin. Chem. Biol.* **2003**, *7*, 166.

CR0206216